

Self-force of a scalar field for circular orbits about a Schwarzschild black hole

Steven Detweiler, Eirini Messaritaki, and Bernard F. Whiting

Department of Physics, P.O. Box 118440, University of Florida, Gainesville, Florida 32611-8440

(Received 20 February 2003; published 21 May 2003)

The foundations are laid for the numerical computation of the actual worldline for a particle orbiting a black hole and emitting gravitational waves. The essential practicalities of this computation are illustrated here for a scalar particle of infinitesimal size and small but finite scalar charge. This particle deviates from a geodesic because it interacts with its own retarded field ψ^{ret} . A recently introduced Green's function G^S precisely determines the singular part ψ^S of the retarded field. This part exerts no force on the particle. The remainder of the field $\psi^R = \psi^{\text{ret}} - \psi^S$ is a vacuum solution of the field equation and is entirely responsible for the self-force. A particular, locally inertial coordinate system is used to determine an expansion of ψ^S in the vicinity of the particle. For a particle in a circular orbit in the Schwarzschild geometry, the mode-sum decomposition of the difference between ψ^{ret} and the dominant terms in the expansion of ψ^S provide a mode-sum decomposition of an approximation for ψ^R from which the self-force is obtained. When more terms are included in the expansion, the approximation for ψ^R is increasingly differentiable, and the mode sum for the self-force converges more rapidly.

DOI: 10.1103/PhysRevD.67.104016

PACS number(s): 04.25.Nx, 04.20.Cv, 04.30.Db, 04.70.Bw

I. INTRODUCTION

In general relativity, a particle of infinitesimal mass will orbit a black hole of large mass along a worldline Γ which is an exact geodesic in the background geometry determined by the large mass alone. If the orbiting particle is not infinitesimal, having a small finite mass, its orbit will no longer be a geodesic in the background of the larger mass, and gravitational waves will be emitted by the system — at infinity. In the neighborhood of the small particle, local measurements cannot separately distinguish the background of the large mass from a *smooth* perturbation to it caused by the presence of the smaller mass [1]. The actual orbit of the particle can be analyzed in a linearization of the Einstein equations via a perturbation expansion in the ratio of the masses. Through first order in this ratio, Γ is known to be a geodesic of a geometry perturbed from the background of the large mass by the presence of the smaller one [1]. The difference of the worldline from a geodesic in the background is said to arise from the interaction of the orbiting particle with its own gravitational field. It is said to result from a “self-force,” even though, in the perturbed geometry determined by both the small and large masses, the orbit would be observed to be geodesic.

In a strict sense, if the particle is of infinitesimal size, then its own field is singular along its worldline, and there the perturbation analysis fails. This difficulty can be avoided by allowing the size of the particle to remain finite while invoking the conservation of the stress-energy tensor within a world tube which surrounds the worldline, in a manner similar to Dirac's [2] classical analysis. The balance of energy and momentum indicates how to calculate the self-force in a way which is independent of the size of the particle. The limit of vanishing size may then be taken without confusion.

In curved spacetime, analyses beginning with DeWitt and Brehme [3] and subsequently by Mino, Sasaki and Tanaka [4] and by Quinn and Wald [5,6] formally resolve the difficulty presented by the singularity in curved spacetime with a

Hadamard expansion [3] of the Green's function near Γ . The retarded Green's function $G^{\text{ret}}(p, p')$ incorporates physically appropriate boundary conditions and describes the field ψ^{ret} of a particle moving through a given spacetime. In most past discussions of the self-force, $G^{\text{ret}}(p, p')$ is commonly divided into a “direct” part, which has support only on the past null cone of the field point p , and a “tail” part, which has support inside the past null cone and is a result of the curvature of spacetime. The analyses show that $\psi^{\text{tail}} = \psi^{\text{ret}} - \psi^{\text{dir}}$ is necessarily finite at the particle and suggest that it is the part of ψ which belongs on the right-hand side of an equation for the self-force [6]

$$\mathcal{F}_a = q \nabla_a \psi. \quad (1)$$

In these approaches, the use of ψ^{tail} instead of ψ^{ret} constitutes a form of regularization of the singular ψ^{ret} . Actually, while finite, ψ^{tail} is generally not differentiable on the worldline [3] if the Ricci scalar of the background is not zero. Similarly, the electromagnetic potential A_a^{tail} (respectively, the gravitational metric perturbation h_{ab}^{tail}) is not differentiable at the particle if $(R_{ab} - \frac{1}{6}g_{ab}R)u^b$ (respectively, $R_{cabd}u^c u^d$) is non-zero in the background. In all such cases, some version of averaging must be invoked to make sense of the self-force. Moreover, we find it instructive to observe that the tail part of the field is necessarily associated with a nonphysical inhomogeneous source, i.e. $\nabla_a \nabla^a \psi^{\text{tail}} \neq 0$: cf. Eq. (30).

In this paper an alternative regularization of the field ψ^{ret} is used to compute the self-force where, in particular, by regularization we mean not only controlling the singular behavior, but also the differentiability. We have recently given a precise procedure for decomposing the retarded field in neighborhood of Γ into two parts [1]:

$$\psi^{\text{ret}} = \psi^S + \psi^R, \quad (2)$$

where ψ^S is a solution of the inhomogeneous field equation for the particle, and is determined in the neighborhood of the

worldline entirely by local analysis via Eq. (36). As both ψ^{ret} and ψ^{S} are inhomogeneous solutions of the same differential equation, it follows that ψ^{R} , defined by Eq. (2) is necessarily a homogeneous solution and is therefore expected to be differentiable on Γ . In Ref. [1] we showed that ψ^{R} formally gives the correct self-force when substituted on the right-hand side of Eq. (1) in place of ψ^{tail} . In this paper ψ^{R} is used for an explicit computation of the self-force. We consider ψ^{S} to be associated with the singular source, and ψ^{R} with the regular remainder.

While the procedure which follows from Eq. (2) is well understood in principle, its application to physically interesting situations remains a challenge. In this paper we consider a particle endowed with a scalar charge q in circular motion about a Schwarzschild black hole. On a technical level, a spherical harmonic decomposition of both ψ^{ret} and ψ^{S} provides the multipole components of each, and the mode by mode sum of the difference of these components determines ψ^{R} and, thence, the self-force.

In Sec. II we give a brief overview of the relation between our work and that of earlier authors. We also summarize our analytical results and introduce the additional regularizing parameters which allow us to obtain increased convergence in our mode sum representation of the self-force.

A special set of coordinates is described in Sec. III; the Thorne-Hartle-Zhang (THZ) coordinates, introduced by Thorne and Hartle [7] and extended by Zhang [8], are locally inertial on a geodesic. These coordinates are convenient for describing the scalar wave equation in the vicinity of the geodesic, where the metric takes a particularly advantageous form. In Sec. IV the Hadamard expansion for the Green's function, discussed in detail by DeWitt and Brehme [3], is described in terms of Synge's [9] "world function" $\sigma(p, p')$, which is defined as half of the square of the geodesic distance between two points p and p' . We obtain both $\sigma(p, p')$ and the Hadamard expansion in terms of the THZ coordinates.

Section V outlines the determination of the regularization parameters given below in Eqs. (13) to (15). These results are in agreement with, but extend by going to higher order, the work of Barack and Ori [10–12] and Mino, Nakano and Sasaki [12,13].

In Sec. VI, with a concrete application of our method, we examine a scalar charge in a circular orbit of the Schwarzschild geometry at a radius of $10M$. It is in this section that we see the practical advantage of using a higher order approximation in the regularization of ψ^{S} . The additional parameters we find enable us to increase dramatically the rate of convergence in the self-force summation.

In several Appendixes we include details concerning the THZ coordinates, the mathematical analyses which focus on calculation of the regularization parameters and a brief summary of details concerning the integration of the scalar wave equation in the Schwarzschild geometry.

Notation. a, b, \dots are four dimensional space-time indices. i, j, \dots are three dimensional spatial indices. (t_s, r, θ, ϕ) are the usual Schwarzschild coordinates. t, x, y, z are locally-inertial THZ coordinates attached to the geodesic Γ , and $\rho^2 \equiv x^2 + y^2 + z^2$. The geodesic Γ is given as x^a

$= z^a(\tau)$, where τ is the proper time along Γ . The flat spatial metric in Cartesian coordinates is δ_{ij} . The flat Minkowski metric in Minkowski coordinates is $\eta_{ab} = (-1, 1, 1, 1)$. The points p and p' refer to a field point and a source point on the world line of the particle, respectively. In the coincidence limit $p \rightarrow p'$. An expression such as $O(\rho^n)$ means of the order of ρ^n as $x^i \rightarrow 0$ in the THZ coordinates. But note that the differentiability of such an order term is only necessarily C^{n-1} at $x^i = 0$.

II. OVERVIEW OF RELATION TO EARLIER WORK

Formally, although our approach differs from that of Barack and Ori, our method of implementation is similar to that in their pioneering analysis in Refs. [10,11,14]. In their procedure, which Burko has implemented [15,16] both for a scalar field with radial and with circular orbits of Schwarzschild, the self-force may be thought of as being evaluated from [30]

$$\mathcal{F}_a^{\text{self}} = \lim_{p \rightarrow p'} [\mathcal{F}_a^{\text{ret}}(p) - \mathcal{F}_a^{\text{dir}}(p)], \quad (3)$$

where p' is the event on Γ where the self-force is to be determined, p is an event in the neighborhood of p' , and the relationship between $\mathcal{F}_a(p)$ and $\psi(p)$ is as given in Eq. (1). To make use of this equation, both $\mathcal{F}_a^{\text{ret}}(p)$ and $\mathcal{F}_a^{\text{dir}}(p)$ are expanded into multipole ℓ modes, with $\mathcal{F}_{\ell a}^{\text{ret}}(p)$ determined numerically. Typically the source is expanded in terms of spherical harmonics, and then a similar expansion for ψ^{ret} is used

$$\psi^{\text{ret}} = \sum_{\ell m} \psi_{\ell m}^{\text{ret}}(r, t) Y_{\ell m}(\theta, \phi) \quad (4)$$

where $\psi_{\ell m}^{\text{ret}}(r, t)$ is found numerically. The individual ℓm components of ψ^{ret} in this expansion are finite at the location of the particle even though their sum is singular. Then $\mathcal{F}_{\ell a}^{\text{ret}}$ is finite and results from summing $q \nabla_a (\psi_{\ell m}^{\text{ret}} Y_{\ell m})$ over m . The ℓ -mode expansion of $\mathcal{F}_a^{\text{dir}}(p)$ was initially determined by a local analysis of the Green's function for an orbit at r_o in Schwarzschild coordinates in Ref. [10],

$$\lim_{r \rightarrow r_o} \mathcal{F}_{\ell a}^{\text{dir}} = \left(\ell + \frac{1}{2} \right) A_a + B_a + \frac{C_a}{\ell + \frac{1}{2}} + O(\ell^{-2}), \quad (5)$$

in which it was found that the $O(\ell^{-2})$ terms yield precisely zero when summed over ℓ . Moreover, for circular geodesics in the equatorial plane of the Schwarzschild geometry, the regularization parameter $C_a = 0$ and A_a and B_a also vanish except for their r components. The values of A_r and B_r , first determined by Barack and Ori [10–12], are given below in Eqs. (13) and (14). A further term, which we shall denote as D'_a , was also introduced in Refs. [10–12] and shown there to be zero. It refers to the sum of the $O(\ell^{-2})$ terms in Eq. (5). We comment further about the contribution of D'_a towards the end of this section. The self-force is ultimately calculated as

$$\mathcal{F}_a^{\text{self}} = \sum_{\ell=0}^{\infty} \left[\lim_{p \rightarrow p'} \mathcal{F}_{\ell a}^{\text{ret}} - \left(\ell + \frac{1}{2} \right) A_a - B_a - \frac{C_a}{\ell + \frac{1}{2}} \right] + D'_a. \quad (6)$$

Burko [15] notes in his numerical analysis that the terms in this sum scale as $1/\ell^2$ for large ℓ , the sum converges as $1/\ell$, and it is evident from his results that he computes to at least $\ell = 80$ and finds improved convergence with Richardson extrapolation.

From our perspective, the self-force at a point p' on Γ is formally given by

$$\mathcal{F}_a^{\text{self}} = \mathcal{F}_a^{\text{ret}} - \mathcal{F}_a^{\text{S}} = \mathcal{F}_a^{\text{R}} \equiv q \nabla_a \psi^{\text{R}} \quad (7)$$

evaluated at the source point p' . Formally, the function ψ^{S} is defined only in a neighborhood of p' ; however for calculational purposes, the function may be extended in any smooth manner throughout the spacetime. While the spherical harmonic components of this extended function in the Schwarzschild geometry are not uniquely determined, they still provide a convergent expression for ψ^{S} for events near p' . Thus, in the Schwarzschild geometry the spherical harmonic expansions of ψ^{S} and ψ^{ret} yield

$$\psi_{\ell m}^{\text{R}}(r, t) = \psi_{\ell m}^{\text{ret}}(r, t) - \psi_{\ell m}^{\text{S}}(r, t), \quad (8)$$

and the self-force can be determined by evaluating the vector field

$$\begin{aligned} \mathcal{F}_a^{\text{self}} &= \nabla_a \sum_{\ell m} \psi_{\ell m}^{\text{R}} Y_{\ell m} \\ &= \nabla_a \sum_{\ell m} (\psi_{\ell m}^{\text{ret}} - \psi_{\ell m}^{\text{S}}) Y_{\ell m} \end{aligned} \quad (9)$$

at the source point p' . Further, with the definitions

$$\mathcal{F}_{\ell a}^{\text{S/ret}} = \nabla_a \sum_m \psi_{\ell m}^{\text{S/ret}} Y_{\ell m}, \quad (10)$$

the self-force is

$$\mathcal{F}_a^{\text{self}} = \sum_{\ell} (\mathcal{F}_{\ell a}^{\text{ret}} - \mathcal{F}_{\ell a}^{\text{S}}) \quad (11)$$

evaluated at r_o . In the above expressions the difference in multipole moments must be taken before the summation over ℓ .

In our approach the regularization parameters are derived from the multipole components of $\nabla_a \psi^{\text{S}}$ evaluated at the source point and are used to control both singular behavior and differentiability. In Sec. V we consider circular orbits of the Schwarzschild geometry at radius r_o and show that

$$\begin{aligned} \lim_{r \rightarrow r_o} \mathcal{F}_{\ell r}^{\text{S}} &= \left(\ell + \frac{1}{2} \right) A_r + B_r - \frac{2\sqrt{2}D_r}{(2\ell-1)(2\ell+3)} \\ &+ \frac{E_r^1 \mathcal{P}_{3/2}}{(2\ell-3)(2\ell-1)(2\ell+3)(2\ell+5)} + \mathcal{O}(\ell^{-6}) \end{aligned} \quad (12)$$

where the regularization parameters are independent of ℓ and given by

$$A_r = -\text{sgn}(\Delta) \frac{[r_o(r_o-3M)]^{1/2}}{r_o^2(r_o-2M)} \quad (13)$$

$$B_r = - \left[\frac{r_o-3M}{r_o^4(r_o-2M)} \right]^{1/2} \left[F_{1/2} - \frac{(r_o-3M)F_{3/2}}{2(r_o-2M)} \right], \quad (14)$$

and

$$\begin{aligned} D_r &= \left[\frac{2r_o^2(r_o-2M)}{r_o-3M} \right]^{1/2} \left[- \frac{M(r_o-2M)F_{-1/2}}{2r_o^4(r_o-3M)} \right. \\ &- \frac{(r_o-M)(r_o-4M)F_{1/2}}{8r_o^4(r_o-2M)} \\ &+ \frac{(r_o-3M)(5r_o^2-7r_oM-14M^2)F_{3/2}}{16r_o^4(r_o-2M)^2} \\ &\left. - \frac{3(r_o-3M)^2(r_o+M)F_{5/2}}{16r_o^4(r_o-2M)^2} \right]. \end{aligned} \quad (15)$$

E_r^1 has not yet been determined analytically, but the constant $\mathcal{P}_{3/2}$ in Eq. (12) is independent of ℓ and is given in Eq. (D23); the ℓ dependence of the E_r^1 term, and of higher order parameters (E_r^k , $k > 1$), is discussed in Sec. V. In these expressions F_q refers to the hypergeometric function ${}_2F_1[q, \frac{1}{2}; 1; M/(r_o-2M)]$. The A_r and B_r terms agree with the results of Refs. [10–13] restricted to circular orbits. When summed over all ℓ , the D_r and E_r^k terms individually give no contribution to the self-force. This is consistent with the results in [10–13], but note the different definition of D_r there, which we have referred to above as D'_a . Our results thus yield the identical self-force to that of Barack and Ori.

As we shall show in Sec. IV, in general ψ^{S} can be known only approximately. If we ignore the D_r and E_r^k terms in the approximation for ψ^{S} , then the approximation for ψ^{R} is only \mathcal{C}^1 . Hence, the D_r and E_r^k terms must be included for ψ^{R} to be a homogeneous solution of Eq. (30) as discussed above. Although we have just indicated above that the D_r and E_r^k terms give no overall contribution to the self-force, we find that understanding the nature of these additional terms can be used to speed up dramatically the convergence of the sum in Eq. (11). We have used this understanding in obtaining the results of Sec. VI.

III. THZ NORMAL COORDINATES

The scalar wave equation takes a simple form when written in a particular coordinate system in which the background geometry looks as flat as possible. Consider a geodesic Γ through a background vacuum spacetime geometry g_{ab} . Let \mathcal{R} be a representative length scale of the background geometry—the smallest of the radius of curvature, the scale of inhomogeneities, and the time scale for changes in curvature along Γ . A *normal* coordinate system can always be found [17] where, on Γ , the metric and its first derivatives match the Minkowski metric, and the coordinate t measures the proper time. Normal coordinates for a geodesic are not unique, and we use particular coordinates which were introduced by Thorne and Hartle [7] and extended by Zhang [8] to describe the external multipole moments of a vacuum solution of the Einstein equations. In Appendix A, we give a constructive algorithm for finding these THZ coordinates for any particular geodesic in a vacuum spacetime. In THZ coordinates

$$\begin{aligned} g_{ab} &= \eta_{ab} + H_{ab} \\ &= \eta_{ab} + {}_2H_{ab} + {}_3H_{ab} + O(\rho^4/\mathcal{R}^4), \quad \rho/\mathcal{R} \rightarrow 0, \end{aligned} \quad (16)$$

with

$$\begin{aligned} {}_2H_{ab} dx^a dx^b &= -\mathcal{E}_{ij} x^i x^j (dt^2 + \delta_{kl} dx^k dx^l) \\ &\quad + \frac{4}{3} \epsilon_{kpq} \mathcal{B}^q_{ij} x^p x^i dt dx^k \\ &\quad - \frac{20}{21} \left[\dot{\mathcal{E}}_{ij} x^i x^j x_k - \frac{2}{5} \rho^2 \dot{\mathcal{E}}_{ik} x^i \right] dt dx^k \\ &\quad + \frac{5}{21} \left[x_i \epsilon_{jpp} \dot{\mathcal{B}}^q_{jk} x^p x^k - \frac{1}{5} \rho^2 \epsilon_{pqi} \dot{\mathcal{B}}^q_{j} x^p \right] dx^i dx^j \end{aligned} \quad (17)$$

and

$$\begin{aligned} {}_3H_{ab} dx^a dx^b &= -\frac{1}{3} \mathcal{E}_{ijk} x^i x^j x^k (dt^2 + \delta_{kl} dx^k dx^l) \\ &\quad + \frac{2}{3} \epsilon_{kpq} \mathcal{B}^q_{ij} x^p x^i x^j dt dx^k \\ &\quad + O(\rho^4/\mathcal{R}^4)_{ij} dx^i dx^j, \end{aligned} \quad (18)$$

where η_{ab} is the flat Minkowski metric in the THZ coordinates (t, x, y, z) , ϵ_{ijk} is the flat space Levi-Civita tensor, $\rho^2 = x^2 + y^2 + z^2$ and the indices i, j, k, l, p and q are spatial and raised and lowered with the three dimensional flat space metric δ_{ij} . Note that a term of $O(\rho^4/\mathcal{R}^4)$ is only known to be C^3 in the limit. We call coordinates where H_{ab} matches only Eq. (17) second order THZ coordinates; these coordinates are well defined up to the addition of arbitrary functions of $O(\rho^4/\mathcal{R}^3)$. Third order THZ coordinates match Eq. (16) through the terms in Eq. (18); these are well defined up to the addition of arbitrary functions of $O(\rho^5/\mathcal{R}^4)$. The ex-

ternal multipole moments are spatial, symmetric, tracefree tensors and are related to the Riemann tensor evaluated on Γ by

$$\mathcal{E}_{ij} = R_{itij}, \quad (19)$$

$$\mathcal{B}_{ij} = \epsilon_i^{pq} R_{pqjt}/2, \quad (20)$$

$$\mathcal{E}_{ijk} = [\nabla_k R_{itij}]^{\text{STF}} \quad (21)$$

and

$$\mathcal{B}_{ijk} = \frac{3}{8} [\epsilon_i^{pq} \nabla_k R_{pqjt}]^{\text{STF}} \quad (22)$$

where STF means to take the symmetric, tracefree part with respect to the spatial indices i, j and k . \mathcal{E}_{ij} and \mathcal{B}_{ij} are $O(1/\mathcal{R}^2)$, and \mathcal{E}_{ijk} and \mathcal{B}_{ijk} are $O(1/\mathcal{R}^3)$. The dot denotes differentiation of the multipole moment with respect to t along Γ . That all of the above external multipole moments are tracefree follows from the assumption that the background geometry is a vacuum solution of the Einstein equations.

The THZ coordinates are a specialization of harmonic coordinates, and it is useful to define the ‘‘Gothic’’ form of the metric

$$\mathfrak{g}^{ab} \equiv \sqrt{-g} g^{ab} \quad (23)$$

as well as

$$\bar{H}^{ab} \equiv \eta^{ab} - \mathfrak{g}^{ab}. \quad (24)$$

A coordinate system is harmonic if and only if

$$\partial_a \bar{H}^{ab} = 0. \quad (25)$$

Zhang [8] gives an expansion of \mathfrak{g}^{ab} for an arbitrary solution of the vacuum Einstein equations in THZ coordinates, his Eq. (3.26). The lower order terms of \bar{H}^{ab} in this expansion are

$$\bar{H}^{ab} = {}_2\bar{H}^{ab} + {}_3\bar{H}^{ab} + O(\rho^4/\mathcal{R}^4) \quad (26)$$

where

$$\begin{aligned} {}_2\bar{H}^{tt} &= -2\mathcal{E}_{ij} x^i x^j \\ {}_2\bar{H}^{tk} &= -\frac{2}{3} \epsilon^{kpq} \mathcal{B}_{qi} x_p x^i + \frac{10}{21} \left[\dot{\mathcal{E}}_{ij} x^i x^j x^k - \frac{2}{5} \dot{\mathcal{E}}_i^k x^i \rho^2 \right] \end{aligned} \quad (27)$$

$${}_2\bar{H}^{ij} = \frac{5}{21} \left[x^{(i} \epsilon^{j)pq} \dot{\mathcal{B}}_{qk} x_p x^k - \frac{1}{5} \epsilon^{pq(i} \dot{\mathcal{B}}^{j)}_{q} x_p \rho^2 \right]$$

and

$$\begin{aligned} {}_3\bar{H}^{tt} &= -\frac{2}{3}\mathcal{E}_{ijk}x^i x^j x^k \\ {}_3\bar{H}^{tk} &= -\frac{1}{3}\epsilon^{kpq}\mathcal{B}_{qij}x_p x^i x^j \\ {}_3\bar{H}^{ij} &= O(\rho^4/\mathcal{R}^4). \end{aligned} \quad (28)$$

At linear order in \bar{H}^{ab} , the metric perturbation H_{ab} is the trace reversed version of \bar{H}^{ab} ,

$$H_{ab} = \bar{H}_{ab} - \frac{1}{2}g_{ab}\bar{H}^c{}_c, \quad (29)$$

and Eqs. (16)–(18) are precisely the terms up to $O(\rho^4/\mathcal{R}^4)$ which correspond to Zhang’s [8] expansion.

IV. GREEN’S FUNCTIONS FOR A SCALAR FIELD

The scalar field equation

$$\nabla^2\psi = -4\pi\varrho \quad (30)$$

is formally solved in terms of a Green’s function,

$$\nabla^2 G(p, p') = -(-g)^{-1/2}\delta^4(x_p^a - x_{p'}^a), \quad (31)$$

where p' represents a source point on Γ , and p a nearby field point. The source function for a point charge moving along a worldline Γ , described by $p'(\tau)$, is

$$\varrho(p) = q \int (-g)^{-1/2} \delta^4(p - p'(\tau)) d\tau, \quad (32)$$

where τ is the proper time along the worldline of the particle with scalar charge q . The scalar field of this particle is

$$\psi(p) = 4\pi q \int G[p, p'(\tau)] d\tau. \quad (33)$$

DeWitt and Brehme [3] analyze scalar-field self-force effects by using the Hadamard expansion of the Green’s function. An important quantity is Sygne’s [9] “world function” $\sigma(p, p')$ which is half of the square of the distance along a geodesic between two nearby points p and p' . The usual symmetric scalar field Green’s function is derived from the Hadamard form to be [3]

$$G^{\text{sym}}(p, p') = \frac{1}{8\pi} [u(p, p')\delta(\sigma) - v(p, p')\Theta(-\sigma)] \quad (34)$$

where $u(p, p')$ and $v(p, p')$ are bi-scalars described by DeWitt and Brehme. The $\Theta(-\sigma)$ guarantees that only when p and p' are timelike related is there a contribution from $v(p, p')$.

The retarded and advanced Green’s functions are

$$\begin{aligned} G^{\text{ret}}(p, p') &= 2\Theta[\Sigma(p), p'] G^{\text{sym}}(p, p') \\ G^{\text{adv}}(p, p') &= 2\Theta[p', \Sigma(p)] G^{\text{sym}}(p, p') \end{aligned} \quad (35)$$

where $\Theta[\Sigma(p), p'] = 1 - \Theta[p', \Sigma(p)]$ equals 1 if p' is in the past of a spacelike hypersurface $\Sigma(p)$ that intersects p , and is zero otherwise. The terms in a Green’s function containing u and v are commonly referred to as the “direct” and “tail” parts, respectively.

A second symmetric Green’s function [1]

$$G^{\text{S}}(p, p') = \frac{1}{8\pi} [u(p, p')\delta(\sigma) + v(p, p')\Theta(\sigma)] \quad (36)$$

precisely identifies the part of ψ which is not responsible for the self-force. In particular, the regular remainder

$$\psi^{\text{R}} = \psi^{\text{ret}} - \psi^{\text{S}} \quad (37)$$

is a homogeneous solution of the field equation (30) and completely provides the self-force when put on the right-hand side of Eq. (1) [1].

A. Approximation for ψ^{S}

In this section approximate expansions are derived for G^{S} and ψ^{S} . For a vacuum spacetime ($R_{ab}=0$) which is nearly flat Thorne and Kovács [18] show that

$$u(p, p') = 1 + O(\rho^4/\mathcal{R}^4), \quad (38)$$

their Eqs. (39) and (40), and they evaluate the direct part of the retarded Green’s function to be

$$\begin{aligned} &\frac{1}{4\pi} u(p, p') \delta_{\text{ret}}[\sigma(p, p')] \\ &= \left(\frac{1 + O(\rho^4/\mathcal{R}^4)}{4\pi\dot{\sigma}} \right)_{\tau_{\text{ret}}} \delta(t_p - t_{\text{ret}}), \end{aligned} \quad (39)$$

where the dot denotes a derivative with respect to $t_{p'}$.

We now express $\dot{\sigma}_{\text{ret}}$ in terms of the THZ coordinates to obtain Eq. (47) below. When the source point p' is on Γ , $\sigma(p, p')$ is particularly easy to evaluate in THZ coordinates for p close to p' . Sygne’s [9] “world function” $\sigma(p, p')$ is shown by Thorne and Kovács [18] to be

$$\sigma(p, p') = \frac{1}{2}x^a x^b \left(\eta_{ab} + \int_{\mathcal{C}} H_{ab} d\lambda \right) + O(\rho^6/\mathcal{R}^4), \quad (40)$$

their Eqs. (37) and (38), where the THZ coordinates of p' are $(t_{p'}, 0, 0, 0)$, x^a is the coordinate of the field point p , and the coordinates of the path of integration \mathcal{C} are given by $\zeta^a(\lambda) = \lambda(x^a - t_{p'}\delta_r^a)$ with λ running from 0 to 1. We closely follow the analysis in [18], while using THZ coordinates, and only work through lower orders in ρ/\mathcal{R} .

Given $H_{ab} = {}_2H_{ab} + {}_3H_{ab}$ from Eqs. (17) and (18), the integral of a component of H_{ab} along \mathcal{C} is straightforward. For example,

$$\begin{aligned} \int_C H_{tt} d\lambda &= - \int_C \left(\mathcal{E}_{ij} \xi^i \xi^j + \frac{1}{3} \mathcal{E}_{ijk} \xi^i \xi^j \xi^k \right) d\lambda + O(\rho^4/\mathcal{R}^4) \\ &= - \frac{1}{3} \mathcal{E}_{ij} x^i x^j - \frac{1}{12} \mathcal{E}_{ijk} x^i x^j x^k + O(\rho^4/\mathcal{R}^4). \end{aligned} \quad (41)$$

The other components give similar results. If we define

$$\mathcal{H}_{ab} \equiv \int_C H_{ab} d\lambda, \quad (42)$$

then Synge's world function is

$$\begin{aligned} \sigma(p, p') &= \frac{1}{2} x^a x^b \eta_{ab} + \frac{1}{2} (t_p - t_{p'})^2 \mathcal{H}_{tt} \\ &\quad + (t_p - t_{p'}) x^i \mathcal{H}_{it} + \frac{1}{2} x^i x^j \mathcal{H}_{ij} + O(\rho^6/\mathcal{R}^4), \\ &= - \frac{1}{2} (1 - \mathcal{H}_{tt}) [(t_{p'} - t_p + x^i \mathcal{H}_{it})^2 \\ &\quad - x^i x^j (\eta_{ij} + \mathcal{H}_{ij}) / (1 - \mathcal{H}_{tt})] + O(\rho^6/\mathcal{R}^4). \end{aligned} \quad (43)$$

The second equality depends upon the facts that $\mathcal{H}_{ab} = O(\rho^2/\mathcal{R}^2)$ and that $|t_{p'} - t_p| = O(\rho)$ near the null cone.

With the source point on Γ ,

$$x^i x^j (\eta_{ij} + \mathcal{H}_{ij}) = \rho^2 (1 + \mathcal{H}_{tt}) + O(\rho^6/\mathcal{R}^4) \quad (44)$$

where

$$\rho^2 = x^i x^j \eta_{ij}. \quad (45)$$

The result in Eq. (44) depends upon the detailed nature of ${}_2H_{ij}$ and ${}_3H_{ij}$ in Eqs. (17) and (18) as well as upon the definition of \mathcal{H}_{ij} in Eq. (42).

After the substitution of Eq. (44) into Eq. (43), factorization of σ yields

$$\begin{aligned} \sigma(p, p') &= - \frac{1}{2} (1 - \mathcal{H}_{tt}) [t_{p'} - t_p + x^i \mathcal{H}_{it} - \rho(1 + \mathcal{H}_{tt})] \\ &\quad \times [t_{p'} - t_p + x^i \mathcal{H}_{it} + \rho(1 + \mathcal{H}_{tt})] + O(\rho^6/\mathcal{R}^4). \end{aligned} \quad (46)$$

At the retarded time, p' is on the past null cone emanating from p , where $\sigma(p, p') = 0$, and it follows that the first of the factors in square brackets is $\sim \rho$ and the second must be $\rho^{-1} \times O(\rho^6/\mathcal{R}^4) = O(\rho^5/\mathcal{R}^4)$ to cancel the order term in Eq. (46) and have $\sigma(p, p')$ vanish precisely. Thus, differentiation of Eq. (46) with respect to $t_{p'}$ and evaluation at the retarded time yields an expression which is dominated by the part which results from the differentiation of the second term in square brackets,

$$\begin{aligned} \left[\frac{d\sigma(p, p')}{dt_{p'}} \right]_{\text{ret}} &= - \frac{1}{2} (1 - \mathcal{H}_{tt}) [t_{p'} - t_p + x^i \mathcal{H}_{it} - \rho(1 + \mathcal{H}_{tt})] \\ &\quad + O(\rho^6/\mathcal{R}^5) \\ &= - \frac{1}{2} (1 - \mathcal{H}_{tt}) [-2\rho(1 + \mathcal{H}_{tt}) + O(\rho^5/\mathcal{R}^4)] \\ &= \rho [1 + O(\rho^4/\mathcal{R}^4)]; \end{aligned} \quad (47)$$

the first equality follows from taking the derivative of the second term in square brackets in Eq. (46) with respect to $t_{p'}$, the second equality from evaluating at the retarded time, and the third equality follows from Eqs. (41) and (42).

The direct part of the retarded Green's function in Eq. (39) is now

$$\begin{aligned} \frac{1}{4\pi} u(p, p') \delta_{\text{ret}}[\sigma(p, p')] \\ &= (4\pi\rho)^{-1} \delta[t_{p'} - t_p + x^i \mathcal{H}_{it} + \rho(1 + \mathcal{H}_{tt}) \\ &\quad + O(\rho^5/\mathcal{R}^4)] [1 + O(\rho^4/\mathcal{R}^4)]. \end{aligned} \quad (48)$$

DeWitt and Brehme show that in general

$$v(p, p') = - \frac{1}{12} R(p') + O(\rho/\mathcal{R}^3), \quad p \rightarrow \Gamma, \quad (49)$$

but in vacuum, where $R=0$ from the Einstein equations,

$$v(p, p') = O(\rho^2/\mathcal{R}^4). \quad (50)$$

This follows from Eq. (2.9) with substitutions from Eqs. (2.14), (2.15), (1.76) and (1.10) of Ref. [3]. The dominant contribution to ψ^S from the $v(p, p')$ term is $O(\rho^3/\mathcal{R}^4)$ in the coincidence limit, $p \rightarrow \Gamma$.

All together then, with Eqs. (48) and (49), substituted into Eq. (36) and an integration over the worldline,

$$\psi^S = q/\rho + O(\rho^3/\mathcal{R}^4). \quad (51)$$

We note that the third order THZ coordinates are only well defined up to the addition of a term of $O(\rho^5/\mathcal{R}^4)$. Such an addition would change $1/\rho$ by the sum of a term that is $O(\rho^3/\mathcal{R}^4)$, and would be consistent with the order term of Eq. (51). The differentiability of the order term is of interest, and a term of $O(\rho^3/\mathcal{R}^4)$ is C^2 in the limit that $\rho \rightarrow 0$. In light of the fact that ψ^R is a homogeneous solution, Eq. (51) clarifies the relationship between the accuracy of an approximation for ψ^S and the differentiability of the subsequent approximation for $\psi^R = \psi^{\text{ret}} - \psi^S$, and the self-force $\partial_a \psi^R$. Specifically, if the approximation for ψ^S is in error by a C^n function, then the approximation for ψ^R is no more differentiable than C^n and the approximation for $\partial_a \psi^R$ is no more differentiable than C^{n-1} .

B. Intuitive understanding for ψ^S

Before continuing, it is instructive to provide an elementary, direct explanation of Eq. (51) by taking full advantage of the features of the THZ coordinates. The scalar wave operator in THZ coordinates, is

$$\sqrt{-g}\nabla^a\nabla_a\psi = \partial_a(\eta^{ab}\partial_b\psi) - \partial_a(\bar{H}^{ab}\partial_b\psi) \quad (52)$$

or

$$\begin{aligned} \sqrt{-g}\nabla^a\nabla_a\psi = & \eta^{ab}\partial_a\partial_b\psi - \bar{H}^{ij}\partial_i\partial_j\psi - 2\bar{H}^{it}\partial_{(i}\partial_{t)}\psi \\ & - \bar{H}^{tt}\partial_t\partial_t\psi. \end{aligned} \quad (53)$$

Direct substitution into Eq. (53) shows how well q/ρ approximates ψ^S . If ψ is replaced by q/ρ on the right hand side, then the first term gives a δ function, the third and fourth terms vanish because ρ is independent of t , and in the second term ${}_2\bar{H}^{ij}$ has no contribution because of the details given in Eq. (27), and the remainder of \bar{H}^{ij} yields a term that scales as $O(\rho/\mathcal{R}^4)$. Thus,

$$\sqrt{-g}\nabla^a\nabla_a(q/\rho) = -4\pi q\delta^3(x^i) + O(\rho/\mathcal{R}^4), \quad \rho/\mathcal{R} \rightarrow 0. \quad (54)$$

From consideration of solutions of Laplace's equation in flat spacetime, it follows that a C^2 correction to q/ρ , of $O(\rho^3/\mathcal{R}^4)$, would remove the remainder on the right-hand side. We conclude that $\psi^S = q/\rho + O(\rho^3/\mathcal{R}^4)$ is an inhomogeneous solution of the scalar field wave equation. And the error in the approximation of ψ^S by q/ρ is C^2 .

V. REGULARIZATION PARAMETERS FOR A CIRCULAR ORBIT OF THE SCHWARZSCHILD GEOMETRY

In Appendix B we give the detailed functional relationship between the THZ coordinates (t, x, y, z) and the Schwarzschild coordinates (t_s, r, θ, ϕ) for an orbit described by $r = r_o$ with $\theta = \pi/2$ and $\phi = \Omega t_s$.

As seen in Sec. IV, an approximation to ψ^S is

$$\psi^S = q/\rho + O(\rho^3/\mathcal{R}^4). \quad (55)$$

The regularization parameters result from evaluating the multipole components of q/ρ at the location of the source. The use in this manner of q/ρ , in lieu of ψ^S itself, is justified because the error in the approximation to ψ^S , being $O(\rho^3/\mathcal{R}^4)$, gives no contribution to $\nabla_a\psi^S$ as $x \rightarrow 0$.

To aid in the multipole expansion we rotate the usual Schwarzschild coordinates to move the coordinate location of the particle from the equatorial plane to a location where $\sin\Theta = 0$ for a specific t_s , following the approach of Barack and Ori as described in [11]. Thus, we define new angles Θ and Φ in terms of the usual Schwarzschild angles by

$$\begin{aligned} \sin\theta\cos(\phi - \Omega t_s) &= \cos\Theta \\ \sin\theta\sin(\phi - \Omega t_s) &= \sin\Theta\cos\Phi \\ \cos\theta &= \sin\Theta\sin\Phi. \end{aligned} \quad (56)$$

A coordinate rotation maps each $Y_{\ell m}(\theta, \phi)$ into a linear combination of the $Y_{\ell m'}(\Theta, \Phi)$ which preserves the index ℓ , while m' runs over $-\ell \dots \ell$. Thus, the ℓ component of the self-force, after summation over m , is invariant under the coordinate rotation.

To obtain the regularization parameters: first we expand $\partial_r(q/\rho)$ into a sum of spherical harmonic components whose amplitudes depend upon r . Then we take the limit $r \rightarrow r_o$. Finally only the $m=0$ components contribute to the self-force at $\Theta=0$ because $Y_{\ell m}(0, \Phi) = 0$ for $m \neq 0$. Thus, the regularization parameters of Eq. (12) are the $(\ell, m=0)$ spherical harmonic components of $\partial_r(q/\rho)$ evaluated at r_o .

In this section ϵ is a formal parameter which is to be set to unity at the end of a calculation; a term containing a factor of ϵ^n is $O(\rho^n)$. We use it to help identify the behavior of certain terms in the coincidence limit, $x^i \rightarrow 0$. We have used MAPLE and GRTENSOR extensively to obtain the results reported below.

A lengthy expression for ρ^2 , for a circular orbit in the Schwarzschild geometry, may be derived from the analysis of Appendix B. The $O(\epsilon^2)$ part of ρ^2 is

$$\tilde{\rho}^2 \equiv \frac{r_o\Delta^2}{r_o - 2M} + 2r_o^2 \frac{r_o - 2M}{r_o - 3M} \chi(1 - \cos\Theta) \quad (57)$$

where

$$\Delta \equiv (r - r_o), \quad (58)$$

and

$$\chi \equiv 1 - \frac{M \sin^2\Phi}{r_o - 2M}. \quad (59)$$

The dependence of ρ^2 on the Schwarzschild coordinates may be written solely in terms of Δ , χ and $\tilde{\rho}$ by use of Eq. (57) to remove $\cos\Theta$, then Eqs. (58) and (59) remove r and $\sin\Phi$ respectively. We formally expand $\partial_r(1/\rho)$ in powers of ϵ to obtain

$$\begin{aligned} \partial_r(1/\rho) = & -\frac{\epsilon^{-2}r_o\Delta}{\tilde{\rho}^3(r_o - 2M)} - \frac{\epsilon^{-1}}{\tilde{\rho}r_o} \left[1 - \frac{r_o - 3M}{2\chi(r_o - 2M)} \right. \\ & + O(\Delta^2/\tilde{\rho}^2, \Delta^4/\tilde{\rho}^4) \left. \right] + \epsilon^0 O(\Delta/\tilde{\rho}, \Delta^2/\tilde{\rho}^2) \\ & + \frac{\epsilon^1\tilde{\rho}}{r_o^4} \left[-\frac{M(r_o - 2M)}{2(r_o - 3M)} - \frac{(r_o - M)(r_o - 4M)}{8\chi(r_o - 2M)} \right. \\ & + \frac{(r_o - 3M)(5r_o^2 - 7r_oM - 14M^2)}{16\chi^2(r_o - 2M)^2} \\ & \left. - \frac{3(r_o - 3M)^2(r_o + M)}{16\chi^3(r_o - 2M)^2} + O(\Delta^2/r_o, \Delta^4/\tilde{\rho}^2r_o) \right] \\ & + O(\rho^2). \end{aligned} \quad (60)$$

We consider the multipole expansion, in the limit that $\Delta \rightarrow 0$, of the $m=0$ part of each coefficient of ϵ^n for $n = -2$ to

1. A convenient method to find the $m=0$ component in one of the following terms involves integrating over the angle Φ using details described in Appendix C. The expansion of the Θ dependence in terms of Legendre polynomials is described in Appendix D.

First term. The $\Delta \rightarrow 0$ limit of the expansion of the ϵ^{-2} term in Eq. (60) is

$$\begin{aligned} & \lim_{\Delta \rightarrow 0} - \frac{\epsilon^{-2} r_o \Delta}{\tilde{\rho}^3 (r_o - 2M)} \\ &= \lim_{\Delta \rightarrow 0} - \left(\frac{r_o}{r_o - 2M} \right)^{1/2} \left(\frac{r_o \Delta^2}{r_o - 2M} \right)^{1/2} \\ & \quad \times \left[\frac{r_o \Delta^2}{r_o - 2M} + \frac{2r_o^2 (r_o - 2M)}{r_o - 3M} \chi (1 - \cos \Theta) \right]^{-3/2} \\ &= - \left(\frac{r_o}{r_o - 2M} \right)^{1/2} \frac{\text{sgn}(\Delta) (r_o - 3M)}{r_o^2 (r_o - 2M - M \sin^2 \Phi)} \\ & \quad \times \sum_{\ell=0}^{\infty} \left(\ell + \frac{1}{2} \right) P_{\ell}(\cos \Theta), \end{aligned} \quad (61)$$

where ϵ has been set equal to 1 on the right-hand side here and below, and where the second equality follows from Eq. (D12) with the substitution

$$\delta^2 = \Delta^2 (r_o - 3M) / [2r_o (r_o - 2M)^2 \chi]. \quad (62)$$

Integrating over Φ and dividing by 2π (denoted by the angle brackets $\langle \rangle$ here and in Appendix C) via Eq. (C7), to find the $m=0$ contribution, results in

$$\begin{aligned} & \lim_{\Delta \rightarrow 0} \left\langle - \frac{\epsilon^{-2} r_o \Delta}{\tilde{\rho}^3 (r_o - 2M)} \right\rangle \\ &= - \text{sgn}(\Delta) \frac{[r_o (r_o - 3M)]^{1/2}}{r_o^2 (r_o - 2M)} \sum_{\ell=0}^{\infty} \left(\ell + \frac{1}{2} \right) P_{\ell}(\cos \Theta). \end{aligned} \quad (63)$$

In the coincidence limit $P_{\ell}(\cos \Theta) = 1$ and a term in this sum is then

$$- \left(\ell + \frac{1}{2} \right) \text{sgn}(\Delta) \frac{[r_o (r_o - 3M)]^{1/2}}{r_o^2 (r_o - 2M)} \quad (64)$$

which determines the A_r term in Eq. (12) as given in Eq. (13).

Second term. The $\Delta \rightarrow 0$ limit of the ϵ^{-1} term in Eq. (60) is

$$\begin{aligned} & \lim_{\Delta \rightarrow 0} - \frac{\epsilon^{-1}}{\tilde{\rho} r_o} \left[1 - \frac{r_o - 3M}{2\chi (r_o - 2M)} \right] \\ &= - \left[\frac{r_o - 3M}{2r_o^4 (r_o - 2M - M \sin^2 \Phi) (1 - \cos \Theta)} \right]^{1/2} \\ & \quad \times \left[1 - \frac{r_o - 3M}{2\chi (r_o - 2M)} \right] \\ &= - \left[\frac{r_o - 3M}{2r_o^4 (r_o - 2M)} \right]^{1/2} \\ & \quad \times (1 - \cos \Theta)^{-1/2} \left[\frac{1}{\chi^{1/2}} - \frac{r_o - 3M}{2\chi^{3/2} (r_o - 2M)} \right]. \end{aligned} \quad (65)$$

Integrating over Φ results in hypergeometric functions as shown in Eq. (C3), and the expansion of $(1 - \cos \Theta)^{-1/2}$ in terms of the $P_{\ell}(\cos \Theta)$ is given in Eq. (D7) and results in

$$\begin{aligned} & \lim_{\Delta \rightarrow 0} \left\langle - \frac{\epsilon^{-1}}{\tilde{\rho} r_o} \left[1 - \frac{r_o - 3M}{\chi (r_o - 2M)} \right] \right\rangle \\ &= - \left[\frac{r_o - 3M}{2r_o^4 (r_o - 2M)} \right]^{1/2} \left[F_{1/2} - \frac{(r_o - 3M) F_{3/2}}{2(r_o - 2M)} \right] \\ & \quad \times \sqrt{2} \sum_{\ell=0}^{\infty} P_{\ell}(\cos \Theta). \end{aligned} \quad (66)$$

In the coincidence limit $P_{\ell}(\cos \Theta) = 1$ and a term in this sum is then

$$B_r = - \left[\frac{r_o - 3M}{r_o^4 (r_o - 2M)} \right]^{1/2} \left[F_{1/2} - \frac{(r_o - 3M) F_{3/2}}{2(r_o - 2M)} \right] \quad (67)$$

which is the B_r term in Eq. (12) as given in Eq. (14).

Third term. The $O(\epsilon^0)$ term in Eq. (60) is zero in the limit that $\Delta \rightarrow 0$ for nonzero Θ , and gives no contribution to the sum in Eq. (12) as follows from Eq. (D7).

Last term. For the last, ϵ^1 , term in Eq. (60) we consider

$$\lim_{\Delta \rightarrow 0} \tilde{\rho} = \left[\frac{2r_o^2 (r_o - 2M)}{r_o - 3M} \right]^{1/2} \chi^{1/2} (1 - \cos \Theta)^{1/2}. \quad (68)$$

After the expansion of $(1 - \cos \Theta)^{1/2}$ described in Eq. (D16) and the integration over Φ with Eq. (C3), the multipole expansion of the $\tilde{\rho}$ terms in Eq. (60) gives

$$\begin{aligned} & \left[\frac{2r_o^2 (r_o - 2M)}{r_o - 3M} \right]^{1/2} \left[- \frac{M (r_o - 2M) F_{-1/2}}{2r_o^4 (r_o - 3M)} \right. \\ & \quad - \frac{(r_o - M) (r_o - 4M) F_{1/2}}{8r_o^4 (r_o - 2M)} \\ & \quad \left. + \frac{(r_o - 3M) (5r_o^2 - 7r_o M - 14M^2) F_{3/2}}{16r_o^4 (r_o - 2M)^2} \right] \end{aligned}$$

$$\begin{aligned}
 & - \frac{3(r_o - 3M)^2(r_o + M)F_{5/2}}{16r_o^4(r_o - 2M)^2} \Bigg] \\
 & \times \sum_{\ell=0}^{\infty} \frac{-2\sqrt{2}P_{\ell}(\cos \Theta)}{(2\ell - 1)(2\ell + 3)}. \quad (69)
 \end{aligned}$$

In the coincidence limit $P_{\ell}(\cos \Theta) = 1$, and a term in this sum is then

$$D_r \frac{-2\sqrt{2}}{(2\ell - 1)(2\ell + 3)}, \quad (70)$$

which defines D_r , as in Eq. (15), and is a term in Eq. (12).

The remainder. These derivations of the regularization parameters reveal a pattern for the ℓ -dependence of higher order parameters, even if the overall scale of the parameter remains unknown.

The successive terms in Eq. (60) provide increasingly accurate approximations of $\partial_r \psi^S$ and also increasingly accurate approximations of $\partial_r \psi^R = \partial_r \psi^{\text{ret}} - \partial_r \psi^S$. In principle the terms through $O(\epsilon^0)$ are sufficient to calculate the radial component of the self-force; this is effectively the level of approximation described in Refs. [10–13] and implemented in Ref. [15]. With the inclusion of $O(\epsilon^0)$ terms the approximation for $\partial_r \psi^R$ is C^0 , the remainder terms scale as ℓ^{-2} for large ℓ and their sum converges. But when the approximation of $\partial_r \psi^S$ is improved by the addition of the $O(\epsilon)$ terms, the resulting approximation of $\partial_r \psi^R$ is then C^1 , and we see below that the remainder terms scale as ℓ^{-4} resulting in a more rapid convergence of the sum for the self-force.

As the approximation of $\partial_r \psi^S$ is improved by successive terms of greater differentiability, the resulting approximation of $\partial_r \psi^R$ is not only more differentiable but also leads to increasingly rapid convergence of the sum for the self-force.

We can anticipate the details of how this occurs. From the descriptions of the THZ coordinates in Appendix B and of ψ^S in terms of THZ coordinates in Sec. IV, we expect that the $O(\epsilon^2)$ term in Eq. (60) is C^1 . A more accurate approximation to ψ^S could be provided by the modification

$$\rho^2 \rightarrow \rho^2 + \lambda_N \mathcal{X}^N, \quad (71)$$

where the components of $\lambda_N = O(1/\mathcal{R}^{n-2})$ are not functions of the coordinates but depend only upon the orbit and the coordinate location of the particle. Here we borrow the notation of the analysis of STF tensors [19] where N is a multi-index that represents n spatial indices $i_1 i_2 \dots i_n$, however while λ_N is symmetric it is not necessarily tracefree. Also \mathcal{X}^N represents $\mathcal{X}^{i_1} \mathcal{X}^{i_2} \dots \mathcal{X}^{i_n}$ where the \mathcal{X}^i represents one of \mathcal{X} , \mathcal{Y} or \mathcal{Z} defined in Appendix B. Now, ρ^2 is already determined through $O(\epsilon^5)$, so that n is necessarily greater than or equal to 6 for an improved approximation. And while we do not know the actual value of λ_N , we assume that such a λ_N exists that provides an improved approximation to ψ^S .

Such a correction to ρ^2 ultimately results in the addition of

$$\partial_r \left[-\frac{\lambda_N \mathcal{X}^N}{2\tilde{\rho}^3} + O(\rho^4/\mathcal{R}^5) \right] \quad (72)$$

to $\partial_r(1/\rho)$ in Eq. (60), which is of $O(\epsilon^2)$ and C^1 if $n=6$. This result is consistent with Eq. (51) and with the discussion following Eq. (54) in Sec. IV above. With this improved approximation the resulting error term in Eq. (60) would be $O(\epsilon^3)$ and C^2 .

Finding higher order THZ coordinates might not be the best way to correct the approximation for ψ^S , but any such correction involving an expansion about Γ would necessarily take the generic form of a homogeneous polynomial in \mathcal{X} , \mathcal{Y} and \mathcal{Z} (or equivalently in x^i) divided by $\tilde{\rho}$ raised to some integral power. Thus to find higher order corrections to ψ^S , we are led to consider the multipole expansion of a term such as in Eq. (72), for $n \geq 6$ and to determine the nature of the regularization parameters that would result.

First \mathcal{X} , \mathcal{Y} and \mathcal{Z} are replaced by their definitions in terms of the usual Schwarzschild coordinates in Eqs. (B1)–(B3). Then, the angles are changed to Θ and Φ via Eq. (56). And finally all coordinate dependence is written in terms of Δ , χ and $\tilde{\rho}$ as described above in Eq. (60). The result is a sum of terms each of which is of $O(\epsilon^{n-4})$, for $n \geq 6$ and whose coordinate dependence is contained in the functions Δ (which depends only upon r), χ (which depends only upon Φ) and $\tilde{\rho}$. As $x \rightarrow 0$ both Δ and $\tilde{\rho}$ are $O(\epsilon)$ while $\chi = O(1)$, so that each term must include a factor $\Delta^q \tilde{\rho}^p$ for integers q and p where $q+p = n-4 \geq 2$. In fact, careful analysis of the above substitutions shows that $q \geq 0$. All of the Θ dependence resides in $\tilde{\rho}^p$.

The Legendre polynomial expansion of $\tilde{\rho}^p$, for odd p , is discussed at length in Appendix D. There we show that when $p = -1$ (respectively, $p < -1$), a consequence of Eq. (D7) [respectively, Eq. (D11)] is that the expansion coefficients scale as a constant (respectively, diverge as $(r-r_o)^p$) when $r \rightarrow r_o$. The coefficients of the expansion $\Delta^q \tilde{\rho}^p$ then scale as $(r-r_o)^q$ [respectively, $(r-r_o)^{q+p}$]. In both cases the power is an integer ≥ 2 . In the limit that $r \rightarrow r_o$ these terms approach zero and give no contribution to the regularization parameters. The case of p even and negative gives a similar result, but is not discussed in the Appendix. We conclude that if $p < 0$ then no contribution to the regularization parameters results.

If $p \geq 0$ and $q > 0$ then the Legendre polynomial expansion of $\tilde{\rho}^p$ is well behaved and finite as $r \rightarrow r_o$, but the product $\Delta^q \tilde{\rho}^p$ vanishes in the limit $r \rightarrow r_o$ and gives no contribution to the regularization parameters.

If $q = 0$ and $p \geq 2$ and is even, then the Θ dependence is in the form of a polynomial in $\cos \Theta$ which has an expansion in terms of the Legendre polynomials only up to $P_p(\Theta)$, and because $\tilde{\rho} = 0$ when $r = r_o$ and $\Theta = 0$ the sum of this finite number of terms is zero and gives no contribution to the regularization parameters. This case always results when the improvement to $\partial_r \psi^S$ is $O(\epsilon^n)$ for n being even.

The only remaining case is $q = 0$ and $p > 2$ being a positive odd integer. In the limit that $r \rightarrow 0$, $\tilde{\rho}^p \propto (1 - \cos \Theta)^{p/2}$.

The Legendre polynomial expansion of this function is discussed in detail in Appendix D. We see in Eq. (D22) that, for k a positive integer

$$(1 - \cos \Theta)^{k+1/2} = \sum_{\ell=0}^{\infty} \mathcal{A}_{\ell}^{k+1/2} P_{\ell}(\cos \Theta) \quad (73)$$

where

$$\begin{aligned} \mathcal{A}_{\ell}^{k+1/2} = & (2\ell + 1) \mathcal{P}_{k+1/2} / [(2\ell - 2k - 1)(2\ell - 2k + 1) \dots \\ & \times (2\ell + 2k + 1)(2\ell + 2k + 3)], \end{aligned} \quad (74)$$

for a constant $\mathcal{P}_{k+1/2}$ given in Eq. (D23). When $\Theta = 0$, $P_{\ell}(\cos \Theta) = 1$ and such terms do contribute additional regularization parameters in the mode sum representation of the self-force. This case always results when the improvement to $\partial_r \psi^S$ is $O(\epsilon^n)$ for n being odd.

We now see that every other higher order correction to ψ^S provides an additional regularization parameter. The ℓ dependence is necessarily of the form

$$E_a^k \mathcal{A}_{\ell}^{k+1/2} \quad (75)$$

where E_a^k is independent of ℓ but still undetermined. The first term of this sort, for $k=1$ is included in Eq. (12). It is important to note that for each value of k the sum of these terms from $\ell=0$ to infinity is necessarily zero, and need not be included in the self-force analysis. However we see in the next section that including these additional coefficients dramatically speeds up the convergence of the self-force sum Eq. (11).

VI. APPLICATION

In this section we apply the formalism developed above to determine the self-force \mathcal{F}_r^R for a scalar charge in orbit at $r = 10M$ about a Schwarzschild black hole. In the numerical work we use units where $M=1$ and $q=1$. Appendix E describes the practical details for numerically integrating the scalar wave equation to determine the $\mathcal{F}_{\ell r}^{\text{ret}}$. To compute the self-force, the A_r , B_r and D_r terms must first be removed from $\mathcal{F}_{\ell r}^{\text{ret}}$ as in Eqs. (11) and (12)—a process which determines residuals which fall off as ℓ^{-4} for large ℓ . Removing the contribution of each successive E_r^k improves the falloff of the residuals by an additional two powers of ℓ .

If we have $\mathcal{F}_{\ell r}^{\text{ret}}$ for all ℓ , summing the residuals after removing A_r , B_r and D_r would give us the self-force. With $\mathcal{F}_{\ell r}^{\text{ret}}$ evaluated only for finite ℓ , we must make some attempt to obtain the higher ℓ contributions. To do this we will numerically determine the E_r^k coefficients by fitting the residuals, considered as a function of ℓ , with a linear combination of terms whose ℓ dependence is given by the E_r^k term in Eq. (12) for $k=1$ and by Eq. (75) for integers $k>1$.

A comparison of the integration results, $\mathcal{F}_{\ell r}^{\text{ret}}$, for different values of an accuracy parameter in the numerical routine, revealed that a systematic effect remained in our best data for $\mathcal{F}_{\ell r}^{\text{ret}}$. In order to avoid fitting to that systematic effect, we chose to add to our data a small random component which

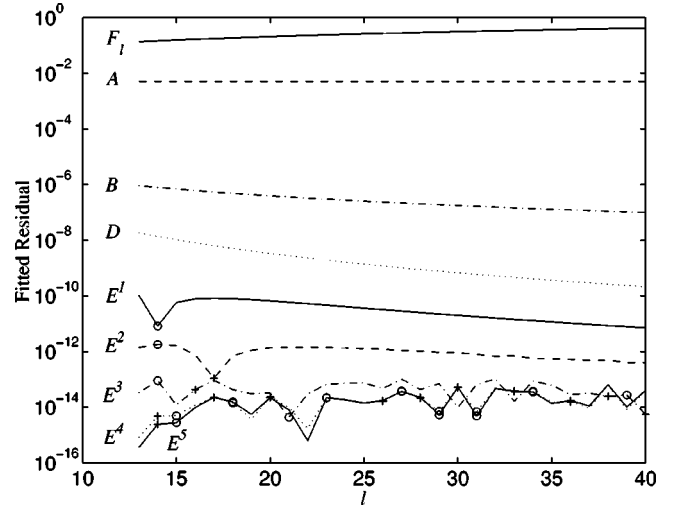


FIG. 1. The upper portion of the figure displays $\mathcal{F}_{\ell r}^{\text{ret}}$ as a function of ℓ , along with the result of it being regularized by A_r , B_r , and D_r . The lower portion displays the residual after a numerical fit of from 1 to 5 additional parameters, $E_r^1 \dots E_r^5$. A point where the data on a particular curve changes sign from being negative to positive is labeled with +, from positive to negative by O.

was capable of swamping any trace of the systematic effect, and which allowed us to have precise control of the error in the $\mathcal{F}_{\ell r}^{\text{ret}}$. This random component also provided the opportunity to use Monte Carlo analysis to determine the statistical significance of our result of the self-force.

In fitting for the E_r^k we avoided small values of ℓ , which may contain significant physical information not associated with the large ℓ falloff of $\mathcal{F}_{\ell r}^{\text{ret}}$. Thus we fitted the residues for ℓ from 13 to 40 while determining from 1 to 5 of the E_r^k coefficients. Figure 1 summarizes the results of this numerical analysis. The curve labeled F_{ℓ} is $\mathcal{F}_{\ell r}^{\text{ret}}$ as a function of ℓ . The curves A , B and D show $\mathcal{F}_{\ell r}^{\text{ret}} - \mathcal{F}_{\ell r}^S$ where $\mathcal{F}_{\ell r}^S$ successively includes the contribution from the regularization parameters A_r , B_r and D_r . The E^1 to E^5 curves show the residuals after numerically fitting from 1 to 5 of the E_r^k coefficients and removing their contributions successively.

We actually used a singular value decomposition from Ref. [20] to fit the residuals. It provided an independent estimate of the uncertainty of the E_r^k 's, which is entirely compatible with the Monte Carlo results. This represented a valuable, overall consistency check of our analysis. The E_r^k coefficients which result from a fit of four coefficients are given in Table I along with their uncertainties in brackets. After fitting four coefficients and removing their contribution, we obtained an rms residual of 2.8×10^{-14} over the

TABLE I. The fitted parameters of $\mathcal{F}_{\ell r}^{\text{ret}}$.

k	E_r^k	E_r^k part of \mathcal{F}_r^R
1	$1.80504(4) \times 10^{-4}$	$2.78201(7) \times 10^{-9}$
2	$-1.000(3) \times 10^{-4}$	$6.90(2) \times 10^{-12}$
3	$4.3(3) \times 10^{-5}$	$3.1(2) \times 10^{-14}$
4	$-5.6(5) \times 10^{-5}$	$7.7(6) \times 10^{-16}$

fitting range, which is completely determined by the size of the random component we had introduced to the original $\mathcal{F}_{\ell r}^{\text{ret}}$ to swamp the systematic effect. Four coefficients evidently fit the data down to the noise. It was clear that fitting a fifth coefficient, or more, did not improve the quality of the fit.

The self-force $\mathcal{F}_r^{\text{R}} = 1.37844828(2) \times 10^{-5}$ was obtained by summing, over the range of our data, $\mathcal{F}_{\ell r}^{\text{ret}}$ with the A_r , B_r and D_r terms removed as in Eqs. (11) and (12). The remainder of the sum to $\ell = \infty$ was approximated by the contributions of the E_r^1, E_r^2, \dots sums from 41 to ∞ , once the E_r^k coefficients had been determined. The uncertainty was obtained from the Monte Carlo simulation. The table also shows the individual contribution of each E_r^k to the self-force \mathcal{F}_r^{R} as well as the amount of the uncertainty in \mathcal{F}_r^{R} which is attributable to that E_r^k . Without including the effects of the E_r^k tails, we would have found the sum out to $\ell = 40$ to be 1.37817×10^{-5} . Fitting the higher order terms has allowed us to increase dramatically the effective convergence to our final result.

Our result is consistent with Fig. (4A) of Burko’s analysis [15]. With the A_r and B_r terms removed from $\mathcal{F}_{\ell r}^{\text{ret}}$, he effectively calculates the total self-force by summing data points on the equivalent of our curve B out to a large enough value of ℓ that convergence is obtained while using Richardson extrapolation.

A future manuscript will apply our methods to the investigation of physical questions.

VII. DISCUSSION

In a previous paper [1], we outlined our method for computing the self-force. This hinged on realizing that $\psi^{\text{R}} = \psi^{\text{ret}} - \psi^{\text{S}}$ is a homogeneous solution of the field equation and we proved that it gave the same result as methods based on using the tail part of the retarded Green’s function. As a consequence of this we have obtained the same regularization parameters as all previous authors [10–13] using a regularization procedure based on mode sum expansions. Exact computation of ψ^{R} would yield a homogeneous solution of the field equation. Under interesting physical circumstances, we anticipate that ψ^{R} should consequently have a high level of differentiability [31]. The level of differentiability of an approximation for ψ^{R} is limited by the accuracy of the approximation for ψ^{S} . To improve the level of differentiability of our approximation for ψ^{R} beyond that of ψ^{tail} , we have thus been led to explore higher order approximations to ψ^{S} .

Following earlier work [21], we have used THZ coordinates to obtain the simple approximation $\psi^{\text{S}} \approx q/\rho$. Our key analytical result is the expansion in Eq. (60) which is based on this approximation. The regularization parameters are derived from the mode sum representation of each term in Eq. (60). The parameters A_r and B_r come from the first two terms. The parameter C_r is seen to be zero, directly from the third term. All these results are consistent with previous work by others [10–13]. Our D_r parameter comes from the fourth term in Eq. (60), which we compute analytically and for which we find the specific ℓ dependence of $1/(2\ell - 1)(2\ell + 3)$. Direct inspection of this term shows that the

sum goes to zero in the coincidence limit, so it does not contribute to the self-force. Nevertheless, it is recognition of the large ℓ behavior of the mode sum expansion for this, and similar higher order terms characterized by the E_r^k , which leads to dramatically improved convergence in the mode summation. Understanding of the specific nature of the ℓ dependence in the mode sum representation of the higher order terms was obtained by an analysis of general methods for improving the approximation to ψ^{S} . Our numerical application of this scheme amply illustrates the benefits of estimating the E_r^k parameters in order to accelerate convergence.

In principle, neither the use of ψ^{R} instead of ψ^{tail} , nor the specific use of THZ coordinates are intrinsically necessary in the computation of the self-force. Indeed, many authors have used neither, and have yet obtained analytical results for the regularization parameters, and/or numerical results for the self-force [10–14,22–24]. It is clear that other methods might also be used to calculate D_r as well as the general ℓ dependence of our E_r^k terms. What we believe is important is that the form of these higher order terms has been determined, and that the inclusion of these terms has a dramatic impact on the effectiveness and accuracy of numerical work.

Unquestionably, the intensity of work in this area is paying off, and as efficient computational techniques are recognized and implemented, a greater volume of results will become available. This will be especially true in relation to the long awaited detection of gravitational waves from binary inspiral sources, represented by a small compact object in orbit about a comparatively large black hole.

ACKNOWLEDGMENTS

The analysis presented in Appendix A was performed by Dong Hoon Kim, and we are grateful to Lior Burko for providing us with some unpublished details of his numerical analysis. This research has been supported in part by the Institute of Fundamental Theory at the University of Florida (E.M), NSF Grant No. PHY-9800977 (B.F.W.) and NASA Grant No. NAGW-4864 (S.D.) with the University of Florida. One of us (B.F.W.) is also grateful to Petr Hájíček and the Swiss National Fonds for the opportunity to visit and work at the University of Bern, Switzerland.

APPENDIX A: THE DETERMINATION OF THZ COORDINATES

A particular THZ coordinate system (t,x,y,z) is associated with any given geodesic $\Gamma(\tau)$ of a vacuum spacetime and is a harmonic coordinate system as well as being “locally inertial and Cartesian.” By Zhang’s [8] definition a “locally inertial and Cartesian” (LIC) coordinate system has the spatial origin $x^i = 0$ on the worldline Γ , and has the metric being expandable about Γ in powers of ρ in a particular form which we describe as $g_{ab} = \eta_{ab} + \rho^p \times$ homogeneous polynomials in x^i of degree q , for non-negative integers p and q with $p + q \geq 2$.

The defining features of n th order THZ coordinates are that

(i) On Γ : t measures the proper time along the geodesic, the spatial coordinates x , y and z are all zero, $g_{ab}|_{\Gamma} = \eta_{ab}$ and all of the first derivatives of g_{ab} vanish.

(ii) At linear, stationary order (cf. Ref. [8]) $\bar{H}^{ij} = O(x^{n+1})$.

(iii) The coordinates satisfy the harmonic gauge condition $\partial_a g^{ab} = O(x^n)$.

To find THZ coordinates associated with a particular geodesic, it is easiest to satisfy these conditions in order.

Given a general set of coordinates Y^A and a particular point p a new set of coordinates X^a may be defined by

$$X^a = A^a + B^a_A (Y^A - Y_p^A) + \frac{1}{2} B^a_A \Gamma^A_{BC} (Y^B - Y_p^B) (Y^C - Y_p^C) + O[(Y - Y_p)^3] Y^A \rightarrow Y_p^A, \quad (\text{A1})$$

where Γ^A_{BC} are the usual Christoffel symbols, the A^a are arbitrary constants, and the B^a_A are also arbitrary constants restricted by the condition that B^a_A , considered a matrix, be invertible. Weinberg [25] shows that

$$g^{ab} = g^{AB} \frac{\partial X^a}{\partial Y^A} \frac{\partial X^b}{\partial Y^B} = \eta^{ab} + O[(Y - Y_p)^2], \quad Y^A \rightarrow Y_p^A, \quad (\text{A2})$$

so that

$$\frac{\partial g^{ab}}{\partial X^c} = O[(Y - Y_p)], \quad Y^A \rightarrow Y_p^A. \quad (\text{A3})$$

A specific choice for the A^a and B^a_A result in the coordinates of p being $X_p^a = \tau_p \delta_t^a$. And condition (i) is satisfied by repeating this construction along Γ while parallel propagating the coordinate basis.

Thus, the coordinates that satisfy condition (i) are denoted X^a . And

$$g^{ab} = \eta^{ab} - \bar{H}^{ab} = \eta^{ab} - \bar{H}^{ab}_{ij} X^i X^j + O(X^3/\mathcal{R}^3), \quad X^i \rightarrow 0, \quad (\text{A4})$$

here X in the order term can refer to any of the spatial coordinates, and the

$$\bar{H}^{ab}_{ij} \equiv \frac{1}{2} \frac{\partial^2 \bar{H}^{ab}}{\partial X^i \partial X^j} \Big|_{\Gamma} \quad (\text{A5})$$

are functions only of t .

To satisfy conditions (ii) and (iii) we use a gauge transformation of the form

$$x^a_{(\text{new})} = X^a_{(\text{old})} + \zeta^a \quad (\text{A6})$$

where changes in geometrical objects are calculated only through linear order in ζ^a . In this application, we are interested in the vicinity of Γ and accordingly let

$$\zeta^a = \zeta^a_{ijk} X^i X^j X^k, \quad (\text{A7})$$

where the ζ^a_{ijk} are functions only of t to be determined below. Thus

$$x^a_{(\text{new})} = X^a + \zeta^a_{ijk} X^i X^j X^k, \quad X^i \rightarrow 0 \quad (\text{A8})$$

changes \bar{H}^{ab} to

$$\bar{H}^{ab}_{\text{new}} = \bar{H}^{ab}_{\text{old}} + \partial^a \zeta^b + \partial^b \zeta^a - \eta^{ab} \partial_c \zeta^c + O(\zeta^2) \quad (\text{A9})$$

or

$$\frac{1}{3} \bar{H}^{abij}_{\text{new}} = \frac{1}{3} \bar{H}^{abij}_{\text{old}} + \zeta^{abij} + \zeta^{baij} - \eta^{ab} \zeta^{kij}. \quad (\text{A10})$$

We find the necessary gauge transformation in two steps. To satisfy condition (ii) we require that the gauge transformation obey

$$\partial^i \zeta^j + \partial^j \zeta^i - \eta^{ij} \partial_c \zeta^c = -\bar{H}^{ij}_{\text{old}} + O(X^3), \quad (\text{A11})$$

which implies that

$$\zeta_{ijkl} + \zeta_{jikl} - \eta_{ij} \zeta^m_{mkl} = -\frac{1}{3} \bar{H}^{\text{old}}_{ijkl}. \quad (\text{A12})$$

We use the decomposition of symmetric trace-free (STF) tensors of Ref. [26] and let

$$\zeta_{ijkl} = A_{\langle ijkl \rangle} + \frac{3}{4} \epsilon_{ip(j} B^p_{kl)} + \frac{5}{7} \delta_{i(j} C_{kl)} - \frac{1}{5} \bar{H}^p_{p(ij} \delta_{kl)}, \quad (\text{A13})$$

where $\langle \dots \rangle$ implies taking the STF part of the enclosed indices and A_{ijkl} , B_{pkl} and C_{kl} are STF tensors on all of their indices. The coefficient $-1/5$ in the last term is chosen to make the trace of Eq. (A13) agree with the trace of Eq. (A12). The remainder of the solution for ζ_{ijkl} is

$$A_{ijkl} = -\frac{1}{6} \bar{H}_{\langle ijkl \rangle} + \frac{1}{7} \delta_{(ij} \bar{H}^p_{kl)p} + \frac{1}{42} \bar{H}^p_{p(ij} \delta_{kl)} - \frac{1}{35} \delta_{(ij} \delta_{jk)} \bar{H}^{pq}_{pq}, \quad (\text{A14})$$

$$B_{pkl} = -\frac{1}{3} \epsilon_{ij(p} \bar{H}^i_{kl)j} + \frac{1}{15} \delta_{(kl} \epsilon_p^{ij} \bar{H}_{ij}^q_{q)}, \quad (\text{A15})$$

and

$$C_{kl} = \frac{1}{3} \bar{H}^i_{ikl} + \frac{1}{15} (\bar{H}^p_{jkp} + \bar{H}^p_{kjp} + \delta_{jk} \bar{H}^{pq}_{pq}), \quad (\text{A16})$$

but only if \bar{H}_{ijkl} satisfies the auxiliary condition that

$$\bar{H}_{kli}^i - \bar{H}^i_{kli} - \bar{H}^i_{lki} + \delta_{kl} \bar{H}^{pq}_{pq} = 0. \quad (\text{A17})$$

This condition is automatically satisfied when \bar{H}^{ab} is derived from a vacuum solution of the Einstein equations, cf. Eq. (35.64) of Ref. [17].

The spatial component of condition (iii) is now satisfied through $O(x)$ because \bar{H}^{ij} vanishes. The time component of condition (iii) will be satisfied through $O(x)$ also if

$$\partial^b \partial_b \zeta^t = -\partial_b \bar{H}_{\text{old}}^{bt}, \quad (\text{A18})$$

thus

$$\begin{aligned} \partial^b \partial_b \zeta^t &= -\ddot{\zeta}^t{}_{ijk} X^i X^j X^k + 6\zeta^t{}_{ik} X^k \\ &= -2\bar{H}^{ti}{}_{ik} X^k + O(X^2) \quad X^i \rightarrow 0, \end{aligned} \quad (\text{A19})$$

or

$$\zeta^t{}_{ik} = -\frac{1}{3}\bar{H}^{ti}{}_{ik}. \quad (\text{A20})$$

An elementary solution for $\zeta^t{}_{ijk}$ is

$$\zeta^t{}_{ijk} = -\frac{1}{5}\bar{H}^{tp}{}_{p(i}\delta_{jk)}. \quad (\text{A21})$$

The combination of Eqs. (A13) and (A21) provides the necessary gauge transformation that results in satisfaction of conditions (ii) and (iii) for second order THZ coordinates.

The third order coordinates may be found following a similar procedure where the gauge transformation is of the form

$$x_{(\text{new})}^a = x_{(\text{old})}^a + \zeta^a{}_{ijkl} X^i X^j X^k X^l, \quad X^i \rightarrow 0. \quad (\text{A22})$$

At the fourth and higher orders, where terms in the metric expansion involving two derivatives of the Riemann tensor

are of the same order as terms quadratic in the Riemann tensor, the presence of nonlinearities complicate the construction of THZ coordinates. We have not needed detailed knowledge about these higher order THZ coordinates throughout this paper.

APPENDIX B: THZ COORDINATES FOR A CIRCULAR ORBIT OF SCHWARZSCHILD

To find the THZ coordinates for a circular orbit in the Schwarzschild geometry it is convenient to take advantage of the spherical symmetry of the background geometry rather than to follow the general procedure described in the preceding section. The orbit Γ , given by $\phi = \Omega t$ where $\Omega = \sqrt{M/r_o^3}$ is the orbital frequency at Schwarzschild radius r_o , is tangent to a Killing vector field $\xi^a \equiv \partial/\partial t_s + \Omega \partial/\partial \phi$. We choose three helping functions \mathcal{X} , \mathcal{Y} and \mathcal{Z} which are Lie derived by the Killing vector, $\mathcal{L}_\xi \mathcal{X} = \mathcal{L}_\xi \mathcal{Y} = \mathcal{L}_\xi \mathcal{Z} = 0$, and their gradients are spatial and orthogonal to the 4-velocity of the geodesic and to each other when evaluated on Γ . These helping functions are

$$\mathcal{X} \equiv \frac{r - r_o}{(1 - 2M/r_o)^{1/2}}, \quad (\text{B1})$$

$$\mathcal{Y} \equiv r_o \sin \theta \sin(\phi - \Omega t_s) \left(\frac{r_o - 2M}{r_o - 3M} \right)^{1/2} \quad (\text{B2})$$

and

$$\mathcal{Z} \equiv r_o \cos(\theta). \quad (\text{B3})$$

Two more useful functions are

$$\begin{aligned} \tilde{x} &= \frac{[r \sin \theta \cos(\phi - \Omega t_s) - r_o]}{(1 - 2M/r_o)^{1/2}} + \frac{M}{r_o^2 (1 - 2M/r_o)^{1/2}} \left[-\frac{\mathcal{X}^2}{2} + \mathcal{Y}^2 \left(\frac{r_o - 3M}{r_o - 2M} \right) + \mathcal{Z}^2 \right] \\ &+ \frac{M\mathcal{X}}{2r_o^3 (r_o - 2M)(r_o - 3M)} [-M^2 \mathcal{X}^2 + \mathcal{Y}^2 (r_o - 3M)(3r_o - 8M) + 3\mathcal{Z}^2 (r_o - 2M)^2] \\ &+ \frac{M}{r_o^5 (1 - 2M/r_o)^{1/2} (r_o - 3M)} \left[M\mathcal{X}^4 \frac{(r_o^2 - r_o M + 3M^2)}{8(r_o - 2M)} + \frac{\mathcal{X}^2 \mathcal{Y}^2}{28} (28r_o^2 - 114r_o M + 123M^2) \right. \\ &+ \frac{\mathcal{X}^2 \mathcal{Z}^2}{14} (14r_o^2 - 48r_o M + 33M^2) + \frac{M\mathcal{Y}^4}{56(r_o - 2M)^2} (3r_o^3 - 74r_o^2 M + 337r_o M^2 - 430M^3) \\ &\left. - \frac{M^2 \mathcal{Y}^2 \mathcal{Z}^2 (7r_o - 18M)}{4(r_o - 2M)} - \frac{M\mathcal{Z}^4}{56} (3r_o + 22M) \right] \end{aligned} \quad (\text{B4})$$

and

$$\begin{aligned} \tilde{y} = & r \sin \theta \sin(\phi - \Omega t_s) \left(\frac{r_o - 2M}{r_o - 3M} \right)^{1/2} + \frac{M\mathcal{Y}}{2r_o^3} \left[-2\mathcal{X}^2 + \mathcal{Y}^2 \left(\frac{r_o - 3M}{r_o - 2M} \right) + \mathcal{Z}^2 \right] + \frac{M\mathcal{X}\mathcal{Y}}{14r_o^5(1-2M/r_o)^{1/2}(r_o-3M)} \\ & \times [2M\mathcal{X}^2(4r_o-15M) + \mathcal{Y}^2(14r_o^2-69Mr_o+89M^2) + 2\mathcal{Z}^2(r_o-2M)(7r_o-24M)]. \end{aligned} \quad (\text{B5})$$

In terms of the functions defined above, the THZ coordinates (t, x, y, z) are

$$x = \tilde{x} \cos(\Omega^\dagger t_s) - \tilde{y} \sin(\Omega^\dagger t_s) \quad (\text{B6})$$

and

$$y = \tilde{x} \sin(\Omega^\dagger t_s) + \tilde{y} \cos(\Omega^\dagger t_s) \quad (\text{B7})$$

where $\Omega^\dagger = \Omega \sqrt{1 - 3M/r_o}$, along with

$$\begin{aligned} z = & r \cos(\theta) + \frac{M\mathcal{Z}}{2r_o^3(r_o-3M)} [-\mathcal{X}^2(2r_o-3M) + \mathcal{Y}^2(r_o-3M) + \mathcal{Z}^2(r_o-2M)] + \frac{M\mathcal{X}\mathcal{Z}}{14r_o^5(1-2M/r_o)^{1/2}(r_o-3M)} \\ & \times [M\mathcal{X}^2(13r_o-19M) + \mathcal{Y}^2(14r_o^2-36r_oM+9M^2) + \mathcal{Z}^2(r_o-2M)(14r_o-15M)] \end{aligned} \quad (\text{B8})$$

and

$$\begin{aligned} t = & t_s(1-3M/r_o)^{1/2} - \frac{r\Omega\mathcal{Y}}{(1-2M/r_o)^{1/2}} + \frac{\Omega M\mathcal{Y}}{r_o^2(1-2M/r_o)^{1/2}(r_o-3M)} \left[-\frac{\mathcal{X}^2}{2}(r_o-M) + M\mathcal{Y}^2 \frac{r_o-3M}{3(r_o-2M)} + M\mathcal{Z}^2 \right] \\ & + \frac{\Omega M\mathcal{X}\mathcal{Y}}{14r_o^3(r_o-2M)(r_o-3M)} [-\mathcal{X}^2(r_o^2-11r_oM+11M^2) + \mathcal{Y}^2(13r_o^2-45r_oM+31M^2) + \mathcal{Z}^2(13r_o-5M)(r_o-2M)]. \end{aligned} \quad (\text{B9})$$

The set of functions $(t, \tilde{x}, \tilde{y}, z)$ forms a noninertial coordinate system that corotates with the particle in the sense that the \tilde{x} axis always lines up the center of the black hole and the center of the particle, the \tilde{y} axis is always tangent to the spatially circular orbit, and the z axis is always orthogonal to the orbital plane. The spatial coordinates are all Lie derived by the Killing vector, $\mathcal{L}_{\tilde{x}}\tilde{x} = \mathcal{L}_{\tilde{y}}\tilde{y} = \mathcal{L}_z z = 0$.

The x^a coordinates (t, x, y, z) are locally inertial and non-rotating in the vicinity of Γ , but these same coordinates appear to be rotating when viewed far from Γ as a consequence of Thomas precession as revealed in the $\Omega^\dagger t_s$ dependence in Eqs. (B6) and (B7) above.

The determination of the THZ coordinates was tedious but not difficult. We looked for the relationship between the THZ coordinates and the usual Schwarzschild coordinates $X^A = (t_s, r, \theta, \phi)$ by using the usual rule for the change in components of a tensor under a coordinate transformation,

$$g^{ab} = g^{AB} \frac{\partial x^a}{\partial X^A} \frac{\partial x^b}{\partial X^B} \quad (\text{B10})$$

where g^{AB} is the Schwarzschild geometry in the Schwarzschild coordinates. The terms through $O(\mathcal{X}^2)$ (the \mathcal{X} in the order term represents any of \mathcal{X} , \mathcal{Y} , or \mathcal{Z}) in the definitions of t , \tilde{x} , \tilde{y} and z and the rotation represented in Eqs. (B6) and

(B7) were chosen so that t measured the proper time on the orbit, $g_{ab}|_\Gamma = \eta_{ab}$ and $\partial_c g_{ab}|_\Gamma = 0$. This much could be done easily by hand and resulted in coordinates that satisfied condition (i) in Appendix A.

The $O(\mathcal{X}^3)$ and $O(\mathcal{X}^4)$ terms were found by use of GRTENSOR running under MAPLE following a procedure similar to that in Appendix A except that we used homogeneous polynomials of the form $\zeta^a_{ijk}\mathcal{X}^i\mathcal{X}^j\mathcal{X}^k$ and $\zeta^a_{ijkl}\mathcal{X}^i\mathcal{X}^j\mathcal{X}^k\mathcal{X}^l$ along with Eq. (B10) to determine $\zeta^a_{ij\dots}$ which resulted in the satisfaction of conditions (ii) and (iii) in Appendix A.

Note that ultimately the THZ coordinates (t, x, y, z) are linear combinations of products of C^∞ functions of the Schwarzschild coordinates, and so are C^∞ functions themselves.

It is convenient to note that the natural Minkowski metric that goes with the Thorne-Hartle coordinates is $\eta_{ab} dx^a dx^b \equiv -dt^2 + dx^2 + dy^2 + dz^2$, while its components in the original Schwarzschild coordinates are

$$\eta_{AB} = \eta_{ab} \frac{\partial x^a}{\partial X^A} \frac{\partial x^b}{\partial X^B}. \quad (\text{B11})$$

Another form for η_{ab} is

$$\eta_{ab} = -\nabla_a t \nabla_b t + \nabla_a x \nabla_b x + \nabla_a y \nabla_b y + \nabla_a z \nabla_b z \quad (\text{B12})$$

or

$$\begin{aligned} \eta_{ab} = & -\nabla_a t \nabla_b t + \nabla_a \tilde{x} \nabla_b \tilde{x} + \nabla_a \tilde{y} \nabla_b \tilde{y} + \nabla_a \tilde{z} \nabla_b \tilde{z} \\ & + (\tilde{x}^2 + \tilde{y}^2) \nabla_a (\Omega^\dagger t_s) \nabla_b (\Omega^\dagger t_s) \\ & + 2[\tilde{x} \nabla_{(a} \tilde{y} - \tilde{y} \nabla_{(a} \tilde{x})] \nabla_b (\Omega^\dagger t_s). \end{aligned} \quad (\text{B13})$$

And from the above definitions it readily follows that $\mathcal{L}_\xi \rho^2 = \mathcal{L}_\xi z = \mathcal{L}_\xi \nabla_a t = 0$, while $\mathcal{L}_\xi x$, $\mathcal{L}_\xi y$, and $\mathcal{L}_\xi t$ are nonzero.

APPENDIX C: INTEGRALS OVER Φ

The approach in this and the following Appendix is similar to that of Appendixes C and D of Ref. [13].

In Sec. V we define

$$\chi \equiv 1 - \alpha \sin^2 \Phi \quad (\text{C1})$$

where

$$\alpha \equiv \frac{M}{r_0 - 2M}. \quad (\text{C2})$$

And we use

$$\begin{aligned} \langle \chi^{-p} \rangle & = \langle (1 - \alpha \sin^2 \Phi)^{-p} \rangle = \frac{2}{\pi} \int_0^{\pi/2} (1 - \alpha \sin^2 \Phi)^{-p} d\Phi \\ & = {}_2F_1\left(p, \frac{1}{2}; 1; \alpha\right) \equiv F_p. \end{aligned} \quad (\text{C3})$$

This result follows almost immediately from

$$\begin{aligned} \langle \chi^{-p} \rangle & = \frac{2}{\pi} \int_0^{\pi/2} (1 - \alpha \sin^2 \Phi)^{-p} d\Phi \\ & = \frac{1}{\pi} \int_0^1 t^{-1/2} (1-t)^{-1/2} (1-\alpha t)^{-p} dt, \end{aligned} \quad (\text{C4})$$

where $t = \sin^2 \Phi$, and from the integral representation of the hypergeometric function, Eq. (15.3.1) of Ref. [27]

$$\begin{aligned} {}_2F_1(a, b; c; z) & = \frac{\Gamma(c)}{\Gamma(b)\Gamma(c-b)} \int_0^1 t^{b-1} (1-t)^{c-b-1} \\ & \quad \times (1-tz)^{-a} dt, \quad \text{Re}(c) > \text{Re}(b) > 0. \end{aligned} \quad (\text{C5})$$

Two elementary special cases of Eq. (C3) are

$$\langle 1 - \alpha \sin^2 \Phi \rangle = {}_2F_1\left(-1, \frac{1}{2}; 1; \alpha\right) = 1 - \frac{1}{2} \alpha = F_{-1} \quad (\text{C6})$$

and

$$\langle (1 - \alpha \sin^2 \Phi)^{-1} \rangle = {}_2F_1\left(1, \frac{1}{2}; 1; \alpha\right) = (1 - \alpha)^{-1/2} = F_1. \quad (\text{C7})$$

The latter is used in Eq. (63) and leads to the A_r term in Eq. (12). The special cases $p = \frac{1}{2}$ and $p = -\frac{1}{2}$ are also easily rep-

resented in terms of complete elliptic integrals of the first and second kinds respectively,

$$\frac{2}{\pi} K(\alpha) = {}_2F_1\left(\frac{1}{2}, \frac{1}{2}; 1; \alpha\right) = F_{1/2} \quad (\text{C8})$$

and

$$\frac{2}{\pi} E(\alpha) = {}_2F_1\left(-\frac{1}{2}, \frac{1}{2}; 1; \alpha\right) = F_{-1/2}. \quad (\text{C9})$$

APPENDIX D: LEGENDRE POLYNOMIAL EXPANSIONS

We require the coefficients $\mathcal{A}_\ell^{p/2}(\delta)$ in the expansion

$$(\delta^2 + 1 - u)^{p/2} = \sum_{\ell=0}^{\infty} \mathcal{A}_\ell^{p/2}(\delta) P_\ell(u), \quad \text{for } \delta \rightarrow 0, \quad (\text{D1})$$

for both positive and negative odd-integral values of p . Note that if p is a positive even integer then the left-hand side is a $p/2$ degree polynomial in u and the sum terminates with $\ell = p$.

First we analyze the negative odd-integral values of p via induction. The generating function for Legendre polynomials is

$$(1 - 2tu + t^2)^{-1/2} = \sum_{\ell=0}^{\infty} t^\ell P_\ell(u), \quad |t| < 1. \quad (\text{D2})$$

With T defined from

$$t = e^{-T}, \quad (\text{D3})$$

Eq. (D2) implies

$$(e^T + e^{-T} - 2u)^{-1/2} = \sum_{\ell=0}^{\infty} e^{-(\ell+1/2)T} P_\ell(u), \quad T > 0. \quad (\text{D4})$$

The expansion

$$e^T + e^{-T} = 2 + T^2 + O(T^4), \quad T \rightarrow 0, \quad (\text{D5})$$

followed by the substitution

$$T = \delta \sqrt{2} \quad (\text{D6})$$

in Eq. (D4) provides

$$\mathcal{A}_\ell^{-1/2} = \sqrt{2} + O(\ell \delta), \quad \delta \rightarrow 0, \quad (\text{D7})$$

which is used in the second term of Eq. (60) to arrive at Eq. (66) and leads to the B_r term of Eq. (12) and to the absence of a term in Eq. (12) which might have resulted from the third term of Eq. (60).

Differentiation of both sides of Eq. (D4) with respect to T yields

$$-\frac{1}{2}(e^T + e^{-T} - 2u)^{-3/2}(e^T - e^{-T}) = \sum_{\ell=0}^{\infty} -\left(\ell + \frac{1}{2}\right) e^{-(\ell+1/2)T} P_{\ell}(u), \quad T > 0. \quad (D8)$$

Simplification and expansion about $T=0$ gives

$$(e^T + e^{-T} - 2u)^{-3/2} = \sum_{\ell=0}^{\infty} \frac{(2\ell+1)}{2T} P_{\ell}(u) [1 + O(\ell T)], \quad T \rightarrow 0, \quad (D9)$$

and repeated differentiation extends this result to

$$(e^T + e^{-T} - 2u)^{-k-1/2} = \sum_{\ell=0}^{\infty} \frac{(2\ell+1)}{2(2k-1)T^{2k-1}} P_{\ell}(u) [1 + O(\ell T)], \quad T \rightarrow 0. \quad (D10)$$

Finally, for $k \geq 1$ the expansion and substitution of Eqs. (D5) and (D6) result in

$$\mathcal{A}_{\ell}^{-k-1/2} = \frac{2\ell+1}{\delta^{2k-1}(2k-1)} [1 + O(\ell \delta)], \quad \delta \rightarrow 0. \quad (D11)$$

For $k=1$

$$\mathcal{A}_{\ell}^{-3/2} = \frac{2\ell+1}{\delta} [1 + O(\ell \delta)], \quad \delta \rightarrow 0, \quad (D12)$$

is used in the first term of Eq. (60) to obtain Eq. (63) and, subsequently, the A_r term of Eq. (12).

Next, for positive odd-integral values of p in Eq. (D1), first let $p=1$ and multiply the left-hand side of Eq. (D2) by $(1-u)^{1/2}$ and the right-hand side by $\sum_{\ell} \mathcal{A}_{\ell}^{1/2} P_{\ell}(u)$. Then, integrate over u from -1 to 1 ; the right-hand side is

$$\sum_{\ell} t^{\ell} \mathcal{A}_{\ell}^{1/2} 2/(2\ell+1) \quad (D13)$$

from the normalization of the Legendre polynomials,

$$\int_{-1}^1 P_{\ell}(u) P_{\ell'}(u) du = \frac{2\delta_{\ell\ell'}}{2\ell+1}. \quad (D14)$$

Now, expand the left-hand side in powers of t to determine the $\mathcal{A}_{\ell}^{1/2}$. This results in

$$(1-u)^{1/2} = \sum_{\ell=0}^{\infty} \frac{-2\sqrt{2}}{(2\ell-1)(2\ell+3)} P_{\ell}(u) \quad (D15)$$

and

$$\mathcal{A}_{\ell}^{1/2} = \frac{-2\sqrt{2}}{(2\ell-1)(2\ell+3)}. \quad (D16)$$

The latter is used in the ϵ^1 term of Eq. (60) to obtain Eq. (69) and, subsequently, the D_r term of Eq. (12).

For other positive odd-integral values of $p > 1$ in Eq. (D1), consider the Legendre polynomial representation of $(1-u)^{k+1/2}$, with k a positive integer,

$$(1-u)^{k+1/2} = \sum_{\ell=0}^{\infty} \mathcal{A}_{\ell}^{k+1/2} P_{\ell}(u) \quad (D17)$$

which defines the expansion coefficients $\mathcal{A}_{\ell}^{k+1/2}$. The first coefficient $\mathcal{A}_0^{k+1/2}$ is obtained by multiplying both sides of Eq. (D17) by $1 = P_0(u)$, integrating over u from -1 to 1 and using the orthogonality of the Legendre polynomials to yield

$$\mathcal{A}_0^{k+1/2} = \frac{2^{k+1/2}}{k + \frac{3}{2}}. \quad (D18)$$

The coefficients $\mathcal{A}_{\ell}^{k+1/2}$ for $\ell \geq 1$ are obtained from Eq. (D15) by induction on k . The derivative of Eq. (D17) provides

$$\begin{aligned} \sum_{\ell=0}^{\infty} \mathcal{A}_{\ell}^{k+1/2} P'_{\ell} &= -\left(k + \frac{1}{2}\right) (1-u)^{k-1/2} \\ &= -\left(k + \frac{1}{2}\right) \sum_{\ell=0}^{\infty} \mathcal{A}_{\ell}^{k-1/2} P_{\ell} \\ &= \left(k + \frac{1}{2}\right) \sum_{\ell=0}^{\infty} \mathcal{A}_{\ell}^{k-1/2} \\ &\quad \times \frac{P'_{\ell-1} - P'_{\ell+1}}{2\ell+1}, \end{aligned} \quad (D19)$$

where the prime denotes differentiation with respect to u , and the last equality follows from Eq. (12.23) of Ref. [28]. A resummation of this last expression yields

$$\begin{aligned} \sum_{\ell=1}^{\infty} \mathcal{A}_{\ell}^{k+1/2} P'_{\ell} &= \left(k + \frac{1}{2}\right) \sum_{\ell=1}^{\infty} \left[\frac{\mathcal{A}_{\ell+1}^{k-1/2}}{2\ell+3} - \frac{\mathcal{A}_{\ell-1}^{k-1/2}}{2\ell-1} \right] P'_{\ell}. \end{aligned} \quad (D20)$$

For $\ell \geq 1$

$$\mathcal{A}_{\ell}^{k+1/2} = \left(k + \frac{1}{2}\right) \left[\frac{\mathcal{A}_{\ell+1}^{k-1/2}}{2\ell+3} - \frac{\mathcal{A}_{\ell-1}^{k-1/2}}{2\ell-1} \right] \quad (D21)$$

provides $\mathcal{A}_{\ell}^{k+1/2}$ in terms of $\mathcal{A}_{\ell}^{k-1/2}$ with the help of Eq. (D18). The final result is

$$\begin{aligned} \mathcal{A}_\ell^{k+1/2} = & \mathcal{P}_{k+1/2}(2\ell+1)/[(2\ell-2k-1) \\ & \times (2\ell-2k+1) \cdots (2\ell+2k+1)(2\ell+2k+3)], \end{aligned} \quad (\text{D22})$$

where

$$\mathcal{P}_{k+1/2} = (-1)^{k+1} 2^{k+3/2} [(2k+1)!!]^2 \quad (\text{D23})$$

for k a positive integer or zero. Equation (D22) is used to furnish the ℓ dependence in the E_r^1 term of Eq. (12).

The significant conclusions of this appendix are summarized in Eqs. (D7), (D11) and (D22).

APPENDIX E: INTEGRATION OF THE SCALAR WAVE EQUATION

The scalar field resulting from a charge q moving in a circular orbit of the Schwarzschild geometry is most easily found following an approach similar to that of Breuer *et al.* [29] or, more recently, Burko [15]. The wave equation for the scalar field is

$$\nabla^2 \psi = -4\pi \varrho, \quad (\text{E1})$$

where the scalar field source ϱ , being distinct from ρ , represents a point charge q moving through spacetime along a worldline $\Gamma(\tau)$, described by coordinates $z^a(\tau)$. This source is

$$\begin{aligned} \varrho(x) = & q \int (-g)^{-1/2} \delta^4(x^a - z^a(\tau)) d\tau \\ = & q (-g)^{-1/2} (dt/d\tau)^{-1} \delta^3(x^i - z^i(t)), \end{aligned} \quad (\text{E2})$$

with τ the proper time along the worldline. For a circular orbit at radius r_o , expanding ϱ in terms of spherical harmonic components provides

$$\begin{aligned} \varrho = & q \int (-g)^{-1/2} \delta(r-r_o) \delta(\theta-\pi/2) \delta(\phi-\Omega t) \\ & \times \delta(t-t(\tau)) d\tau \\ = & r^{-2} q \delta(r-r_o) \delta(\theta-\pi/2) \delta(\phi-\Omega t) dt/d\tau \\ = & \sum_{\ell m} \frac{q_{\ell m}}{4\pi r_o} \delta(r-r_o) e^{i\omega_m t} Y_{\ell m}(\theta, \phi), \end{aligned} \quad (\text{E3})$$

where

$$\omega_m \equiv -m\Omega, \quad (\text{E4})$$

$$q_{\ell m} = \frac{4\pi q}{r_o} \frac{Y_{\ell m}^*(\pi/2, 0)}{dt/d\tau}, \quad (\text{E5})$$

and

$$\frac{dt}{d\tau} = \frac{1}{\sqrt{1-3M/r_o}}. \quad (\text{E6})$$

Also, decomposing ψ provides

$$\psi = \sum_{\ell, m} \psi_{\ell m}(r) e^{i\omega_m t} Y_{\ell m}(\theta, \phi), \quad (\text{E7})$$

and the ℓm component of the scalar wave equation becomes

$$\begin{aligned} \frac{d^2 \psi_{\ell m}}{dr^2} + \frac{2(r-M)}{r(r-2M)} \frac{d\psi_{\ell m}}{dr} + \left[\frac{\omega^2 r^2}{(r-2M)^2} - \frac{\ell(\ell+1)}{r(r-2M)} \right] \psi_{\ell m} \\ = -\frac{q_{\ell m}}{r_o - 2M} \delta(r-r_o). \end{aligned} \quad (\text{E8})$$

We know that

$$Y_{\ell, -m} = (-1)^m Y_{\ell, m}^*, \quad (\text{E9})$$

and the reality of ϱ and of the final solution for $\psi(t, r, \theta, \phi)$ requires similar expressions for $q_{\ell, -m}$ and $\psi_{\ell, -m}$.

The boundary conditions of interest require only ingoing waves at the event horizon

$$\psi_{\ell m} = e^{i\omega r_* / r}, \quad r \rightarrow 2M, \quad (\text{E10})$$

and only outgoing waves at infinity

$$\psi_{\ell m} = e^{-i\omega r_* / r}, \quad r \rightarrow \infty, \quad (\text{E11})$$

where

$$r_* = r + 2M \log(r/2M - 1). \quad (\text{E12})$$

An expansion of $\psi_{\ell m}$ starts the numerical integration at large r . We assume that

$$\psi_{\ell m}(r) = \frac{e^{-i\omega r_*}}{r} \sum_{n=0} \frac{a_n}{r^n} \quad (\text{E13})$$

and, with Eq. (E8), obtain a recursion relation for a_n :

$$a_n = \frac{n(n-1) - \ell(\ell+1)}{2i\omega n} a_{n-1} - \frac{M(n-1)^2}{i\omega n} a_{n-2}, \quad (\text{E14})$$

with the starting values of $a_0 = 1$ and $a_{n<0} = 0$. This is an asymptotic expansion, and we begin the integration of Eq. (E8) at a value of r which is just big enough that the sum in Eq. (E13) reaches machine accuracy before beginning to diverge. We numerically integrate Eq. (E8) in to the radius of the orbit r_o : this provides us with a homogeneous solution ψ^∞ with proper boundary conditions at large r .

Similarly an expansion of $\psi_{\ell m}$ for small $r-2M$ starts the numerical integration near the event horizon. We assume that

$$\psi_{\ell m}(r) = \frac{e^{i\omega r_*}}{r} \sum_{n=0} b_n (r-2M)^n \quad (\text{E15})$$

and, with Eq. (E8), obtain a recursion relation for b_n :

$$\begin{aligned}
 b_n = & -\frac{12i\omega M(n-1) + (2n-3)(n-1) - (\ell^2 + \ell + 1)}{2M(4in\omega M + n^2)} b_{n-1} \\
 & -\frac{12i\omega M(n-2) + (n-2)(n-3) - \ell(\ell+1)}{4M^2(4in\omega M + n^2)} b_{n-2} \\
 & -\frac{i\omega(n-3)}{2M^2(4in\omega M + n^2)} b_{n-3}, \tag{E16}
 \end{aligned}$$

with the starting values of $b_0 = 1$ and $b_{n < 0} = 0$. We begin the integration of Eq. (E8) at a value of $r - 2M$ which is just small enough that the sum in Eq. (E15) reaches machine accuracy within a reasonable number of terms. We numerically integrate Eq. (E8) out to the radius of the orbit r_o : this provides us with a homogeneous solution ψ^H with proper boundary conditions near the event horizon.

The retarded field is

$$\psi_{\ell m}^{\text{ret}} = \begin{cases} A \psi_{\ell m}^H, & r < r_o \\ B \psi_{\ell m}^\infty, & r > r_o, \end{cases} \tag{E17}$$

with the match at r_o determined by the δ -function source of Eq. (E8),

$$\left(B \frac{d\psi_{\ell m}^\infty}{dr} - A \frac{d\psi_{\ell m}^H}{dr} \right)_{r_o} = -\frac{q_{\ell m}}{r_o - 2M} \tag{E18}$$

which yields

$$A \left(\psi_{\ell m}^H \frac{d\psi_{\ell m}^\infty}{dr} - \psi_{\ell m}^\infty \frac{d\psi_{\ell m}^H}{dr} \right) = -\psi_{\ell m}^\infty \frac{q_{\ell m}}{r_o - 2M} \tag{E19}$$

and

$$B \left(\psi_{\ell m}^H \frac{d\psi_{\ell m}^\infty}{dr} - \psi_{\ell m}^\infty \frac{d\psi_{\ell m}^H}{dr} \right) = -\psi_{\ell m}^H \frac{q_{\ell m}}{r_o - 2M}. \tag{E20}$$

The ℓ component of the radial self-force for ψ^{ret} in Eq. (11), is then given by

$$\mathcal{F}_{\ell r}^{\text{ret}} = \sum_{m=-\ell}^{\ell} \left. \frac{d\psi_{\ell m}^{\text{ret}}}{dr} \right|_{r_o}. \tag{E21}$$

Section VI describes the efficient use of $\mathcal{F}_{\ell r}^{\text{ret}}$ in the determination of the self-force.

-
- [1] S. Detweiler and B. F. Whiting, *Phys. Rev. D* **67**, 024025 (2003).
- [2] P. A. M. Dirac, *Proc. R. Soc. London* **A167**, 148 (1938).
- [3] B. S. DeWitt and R. W. Brehme, *Ann. Phys. (N.Y.)* **9**, 220 (1960).
- [4] Y. Mino, M. Sasaki, and T. Tanaka, *Phys. Rev. D* **55**, 3457 (1997).
- [5] T. C. Quinn and R. M. Wald, *Phys. Rev. D* **56**, 3381 (1997).
- [6] T. C. Quinn, *Phys. Rev. D* **62**, 064029 (2000).
- [7] K. S. Thorne and J. B. Hartle, *Phys. Rev. D* **31**, 1815 (1985).
- [8] X.-H. Zhang, *Phys. Rev. D* **34**, 991 (1986).
- [9] J. L. Synge, *Relativity: The General Theory* (North-Holland, Amsterdam, 1960).
- [10] L. Barack and A. Ori, *Phys. Rev. D* **61**, 061502(R) (2000).
- [11] L. Barack and A. Ori, *Phys. Rev. D* **66**, 084022 (2002).
- [12] L. Barack, Y. Mino, H. Nakano, A. Ori, and M. Sasaki, *Phys. Rev. Lett.* **88**, 091101 (2002).
- [13] Y. Mino, H. Nakano, and M. Sasaki, *Prog. Theor. Phys.* **108**, 1039 (2002).
- [14] L. Barack and A. Ori, *Phys. Rev. D* **67**, 024029 (2003).
- [15] L. M. Burko, *Phys. Rev. Lett.* **84**, 4529 (2000).
- [16] L. Barack and L. M. Burko, *Phys. Rev. D* **62**, 084040 (2000).
- [17] C. W. Misner, K. S. Thorne, and J. A. Wheeler, *Gravitation* (Freeman, San Francisco, 1973).
- [18] K. S. Thorne and S. J. Kovács, *Astrophys. J.* **200**, 245 (1975).
- [19] T. Damour and B. R. Iyer, *Ann. I.H.P. Phys. Theor.* **54**, 115 (1991).
- [20] W. H. Press, S. A. Teukolsky, W. T. Vetterling, and B. P. Flannery, *Numerical Recipes in C: The Art of Scientific Computing*, 2nd ed. (Cambridge University Press, Cambridge, England, 1992).
- [21] S. Detweiler, *Phys. Rev. Lett.* **86**, 1931 (2001).
- [22] C. O. Lousto, *Phys. Rev. Lett.* **84**, 5251 (2000).
- [23] C. O. Lousto, *Class. Quantum Grav.* **18**, 3989 (2001).
- [24] L. Barack and C. O. Lousto, *Phys. Rev. D* **66**, 061502(R) (2002).
- [25] S. Weinberg, *Gravitation and Cosmology* (Wiley, New York, 1972).
- [26] T. Damour and B. R. Iyer, *Phys. Rev. D* **43**, 3259 (1991).
- [27] *Handbook of Mathematical Functions*, edited by M. Abramowitz and I. A. Stegun (Dover, New York, 1965).
- [28] G. B. Arfken and H. J. Weber, *Mathematical Methods for Physicists*, 5th ed. (Harcourt/Academic, San Diego, 2001).
- [29] R. A. Breuer, P. L. Chrzanowski, H. G. Hughes III, and C. W. Misner, *Phys. Rev. D* **8**, 4309 (1973).
- [30] We use ψ^{ret} throughout in places where other authors have used ψ^{full} or ψ^{total} to denote the ‘‘actual’’ field [2].
- [31] The differentiability of ψ^R is controlled by boundary conditions and initial data. We consider nondifferentiable initial data or shock waves coming in from boundaries to be physically unreasonable.